Palaeogeography, Palaeoclimatology, Palaeoecology 654 (2024) 112429

Contents lists available at ScienceDirect

Palaeogeography, Palaeoclimatology, Palaeoecology

journal homepage: www.elsevier.com/locate/palaeo

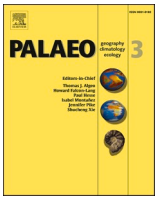

Sclerochronology of the large scallops *Gigantopecten latissimus* and *Pecten jacobaeus* in a Pliocene warmer Mediterranean Sea

Silvia Danise [a,*], Giada Giachetti [a], Ilaria Baneschi [b], Martina Casalini [a], Francesco Miniati [c], Stefano Dominici [d], Chiara Boschi [b]

[a] *Università degli Studi di Firenze, Dipartimento di Scienze della Terra, via La Pira 4, 50121 Firenze, Italy*
[b] *CNR-Istituto di Geoscienze e Georisorse, Via Moruzzi 1, 56127 Pisa, Italy*
[c] *CNR- Istituto di Geoscienze e Georisorse, Via G. La Pira, 4, 50121 Firenze, Italy*
[d] *Università degli Studi di Firenze, Museo di Storia Naturale, via La Pira 4, 50121 Firenze, Italy*

ARTICLE INFO

Editor: Prof. M Elliot

Keywords:
Bivalve
Fossil
Pliocene
Sclerochronology
Seasonality
Isotopes

ABSTRACT

Here we apply a sclerochronological approach to reconstruct the life-history of two stenohaline bivalves of the family Pectinidae, *Gigantopecten latissimus* and *Pecten jacobaeus* from the Pliocene of Italy. The specimens come from the locality of Torrita di Siena (Siena-Radicofani Basin, Tuscany), dated to the late Zanclean-Piacenzian with nannoplankton biostratigraphy and Sr-isotope stratigraphy. After measuring the width of micro-growth increments and verifying that the shells were not diagenetically altered, we sampled them at high resolution for carbon and oxygen stable isotopes. $\delta^{13}C$ and $\delta^{18}O$ shell values allowed to distinguish between specimens that lived above or below the thermocline. Those influenced by surface waters indicate temperatures (for $\delta^{18}O_{seawater}$ = 1.5‰) with winter minima of 16–18 °C and summer values up to 28–29 °C, close to present temperature conditions in the tropical west-African climate belt. In line with this, we found that the two species had similar seasonal growth patterns, with faster growth during colder months and summer slowdown, a typical adaptation of bivalves of tropical affinity suffering from summer temperature extremes. Despite this similar adaptation, *G. latissimus*, with large and heavy shells (length up to 30 cm) became extinct around 3.0 Ma, while the smaller *P. jacobaeus* survived Plio-Pleistocene cooling. Different growth rates between the two species and, therefore, different metabolic costs, might explain such differential response, together with differences in reproduction strategies. Habitat loss and fragmentation, due to the decrease of shelf margins and organogenic substrates caused by cooling and sea level fall, are abiotic factors that could have also contributed to the extinction of *G. latissimus*. *P. jacobaeus* adaptation to live across a larger bathymetric range, which indicates the ability to thrive in a wider range of temperatures, most likely played a role in its survival. Further studies, including more specimens across multiple localities, will help verifying these hypotheses.

1. Introduction

The Mediterranean Sea is presently recognised as a biodiversity hotspot (Coll et al., 2010), and it was more so during the Pliocene, as documented by the molluscs. Species loss occurred between 3.0 and 2.5 Ma and coincided with climate and other environmental changes caused by the intensification of the Northern Hemisphere Glaciation (Monegatti and Raffi, 2001; Danise and Dominici, 2023). Concerning bivalves, around 17% of the species went extinct; extinction was selective, as suspension feeders, both infaunal and epifaunal, were more affected compared to infaunal deposit feeders (Mondanaro et al., 2024). Tropical climate conditions, that for most of the Pliocene extended from southern Portugal to western Africa, at the end of the Pliocene retreated their latitudinal extension to south of the Cape Verde Islands, leaving a warm-temperate climate in the Mediterranean Sea (Silva, da C.M., Landau, B., 2007; Ávila et al., 2016). Most of the extinct species are considered of tropical affinity, and climate cooling is considered the primary cause of extinction (Raffi and Marasti, 1985; Monegatti and Raffi, 2001). Besides that, it has never been directly investigated whether temperature drop was the primary, direct driver of extinction, by physiologically impacting species survival, or if indirect drivers linked to changes in the environment or species interactions had a greater role in biodiversity

* Corresponding author.
E-mail address: silvia.danise@unifi.it (S. Danise).

https://doi.org/10.1016/j.palaeo.2024.112429
Received 27 October 2023; Received in revised form 7 August 2024; Accepted 11 August 2024
Available online 13 August 2024

loss. Plio-Pleistocene extinctions of some large tropical species in the western Atlantic and the Caribbean Sea have been ascribed, for instance, to changes in ocean circulation and primary productivity (Kirby and Jackson, 2004), or to increased predation vulnerability due to slower growth rates caused by climate cooling and reduced productivity (Johnson et al., 2019, 2021a).

Sclerochronology by combining the analysis of bivalve seasonal growth patterns with geochemical proxies, like carbon and oxygen stable isotopes, has the potential to help understand the adaptation of species to climatic conditions (Moss et al., 2016, 2021; Peharda et al., 2021), and its application to Pliocene bivalves can improve our understanding of their possible responses to climate change. Bivalves form their shells at varying rates throughout the year, and this is represented by growth increments and growth lines. Growth increments represent intervals of times in which the organisms produce their shell with fast growth and can provide information on environmental conditions during growth. Growth lines identify periods of very slow growth and/or growth cessation. These can be caused by multiple factors, like genetically encoded biological clocks (e.g. daily growth pattern), other biological processes (e.g. spawning) or abiotic factors, especially temperature and primary production (Schöne and Surge, 2012). Temperature is one of the main controls on growth rate of bivalve shells. It has been observed, for instance, that many modern cold-temperate bivalves inhabiting mid- to high latitudes stop growing preferentially during winter months, whereas those from low latitudes, belonging to tropical and warm-temperate provinces, tend to form annual growth lines during summer months (Killam and Clapham, 2018). Most likely because of its past climate history, the Mediterranean Sea hosts bivalves with both summer and winter shutdown strategies (Killam and Clapham, 2018; Peharda et al., 2019). Furthermore, temperature is one of the most significant abiotic factors in marine ecosystems, affecting almost all aspects of organismal physiology. Hence, adaptation to environmental conditions is considered one of the major challenges in evolutionary adaptation and survival, and is thought to be dependent, to a large extent, on the organism's ability to undergo metabolic reorganization on both short-term and evolutionary time-scales (Heilmayer et al., 2004).

Here we analyse with a sclerochronological approach two species of Pectinidae from the Pliocene of central Italy. Pectinidae are a family of bivalves that suffered high extinction rates through the Plio-Pleistocene interval (Danise and Dominici, 2023). Among the two species, *Gigantopecten latissimus* (Brocchi, 1814) went extinct, and the other, *Pecten jacobaeus*, Linnaeus, 1758, survived and is the largest scallop inhabiting the Mediterranean Sea today. In order to reconstruct the life-history traits of these two organisms we combined the analysis of growth increments and carbon and oxygen stable isotopes from the shell, with the starting hypothesis that different adaptations might have controlled species survival or extinction (e.g. Moss et al., 2021). After discussing the possible biotic and abiotic factors of such differential extinction, we finally use oxygen isotope data to reconstruct seasonal temperatures in the Pliocene of the Tyrrhenian Sea and discuss the challenges of such reconstructions.

2. Geological setting

The studied specimens come from mid-Pliocene sediments of the Siena-Radicofani Basin (Tuscany, Italy, Fig. 1), one of the Neogene-Quaternary intermontane basins of the Northern Apennines, a Tertiary fold-and thrust belt resulting from the collision between the Adria and Corsica-Sardinian microplates, in the larger context of the collision of Africa with Eurasia (Carmignani et al., 2001 and references therein). These basins developed in the westernmost sector of the Northern Apennines starting from the early-middle Miocene as NW to NNW elongated (up to 200 km long) and relatively narrow (up to 25 km wide) morpho-structural depressions, crossed transversely by SW-NE-oriented tectonic lineaments (Martini and Sagri, 1993; Pascucci et al., 2007). The Siena-Radicofani Basin is located east of the Middle-Tuscan Range and extends from the southern part of the Chianti Hills to the northern part of the Vulsini Mountains. It is filled by late Serravallian to Gelasian age continental and marine sediments (Bossio et al., 1993; Martini et al., 2011, 2021) that have been subdivided into four unconformity-bounded stratigraphic units, SU1 (oldest) to SU4 (youngest; Bonini and Sani, 2002). The studied specimens come from unit SU4. Unit SU4 is up to 600 m thick (Bonini and Sani, 2002; Brogi, 2011) and consists of Zanclean-early Gelasian marine deposits with subordinate alluvial sediments. The unit starts with fluvial sandy conglomerates and floodplain organic-rich silty clays grading upward to offshore silty clays overlain by regressive shallow-marine sand and conglomerates (Bossio et al., 1993; Martini and Aldinucci, 2017). Following a regional uplift, the area emerged above sea level in the latest Piacenzian-early Gelasian and was later dissected by fluvial networks (Martini et al., 2016).

The 1.5 m-thick sequence exposed at the investigated outcrop, located close to the town of Torrita di Siena (43°09′30.13″N; 11°47′03.29″E), is made of beds of coarse sand, with gravel and calcilutite pebbles, interbedded with thinner beds of sandy mudstones, all included in the upper, regressive part of unit SU4. Beds range in thickness from 10 to 25 cm. Pebbles, up to 20 cm in length, are often encrusted with balanids and bioeroded by *Gastrochaenolites* borings. The lower part of the outcrop is rich in macro-invertebrates, especially molluscs, including bivalves belonging to the Pectinidae (*G. latissimus, P.*

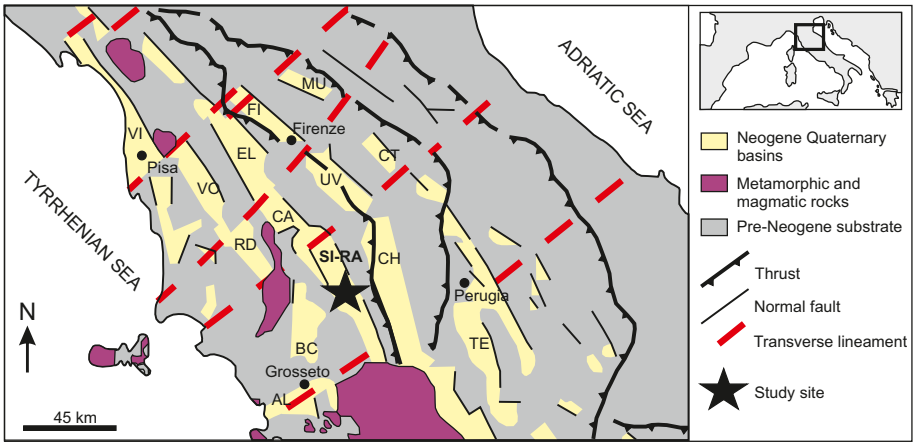

Fig. 1. Location of the Siena-Radicofani Basin, and the locality of Torrita di Siena, with respect to the main Neogene–Quaternary basins of inner northern Apennines. Modified after Ghinassi and Ielpi (2018). Abbreviations of basin names: AL: Albegna, BC: Baccinello, CA: Casino, CH: Chiana, CT: Casentino, EL: Elsa, FI: Firenze, MU: Mugello, RD: Radicondoli, SI-RA: Siena-Radicofani, TE: Tiberino, VI: Viareggio, VO: Volterra, UV: Upper Valdarno.

jacobaeus, *Flabellipecten flabelliformis*, *Aecquipecten opercularis*, *Talochlamys multistriata*, *Mimachlamys varia*, *Flexopecten flexuosus*), Ostreidae (*Ostrea edulis*) and Chamidae (*Chama gryphoides*), scaphopods, gastropods (*Petaloconchus glomeratus*, *Helminthia* sp.) and terebratulid brachiopods (Fig. S1a). The sedimentary facies and the fossil association point to a shoreface setting characterized by sediment starvation and condensation. Finer grained interbeds indicate short-term rises of fair-weather wave base (see Martini and Aldinucci, 2017).

2.1. Ecology and palaeoecology of the species under study

Pectinidae of the extinct genus *Gigantopecten* have inhabited the western Tethys since the late Oligocene (Bongrain, 1992) and the proto-Mediterranean and the Paratethys since the early Miocene (Bongrain, 1992; Harzhauser et al., 2003). Early Miocene species of *Gigantopecten* occupied high-energy, fully marine, shallow-water environments and had large heavy shells (Harzhauser et al., 2003), being preferentially adapted to bioclastic carbonate seafloors and coarse shallow-water siliciclastic environments (Bongrain, 1988; Mandic and Piller, 2001). Their abundance has been related to the presence of extended shelf regions typical of eustatic sea level high-stand conditions and times of global warming (Bongrain, 1988). While some authors attribute some Miocene specimens to *G. latissimus* (e.g. Freneix et al., 1987; Bongrain, 1992), others attribute the Miocene forms to *G. nodosiformis* (see discussion in Studencka, 2019). The undoubted stratigraphic distribution of *G. latissimus* is from the Zanclean to the lower Piacenzian in the Mediterranean Sea (Danise and Dominici, 2023) and the Zanclean in the eastern Atlantic, from the Azores to the Canary Islands (Ávila et al., 2015; Meco et al., 2020). Its extirpation from the Canary Islands, together with other tropical species, occurred around 4.0 Ma, with the establishment of the cool Canary Current and of the Trade Winds from the north (Meco et al., 2020). Its final extinction, involving disappearance from the Mediterranean Sea and the rest of the Atlantic, around 3.0 Ma ago, coincides with the initiation of the cooling related to the Northern Hemisphere Glaciation and the reduction of continental shelf regions (Harzhauser et al., 2003; Danise and Dominici, 2023). During the Zanclean this species mostly occurs in conglomerates, coarse-grained sands, and calcarenites-calcirudites (Jiménez et al., 2009; García-Ramos and Zuschin, 2019). In southern France it reaches a maximum length of 30 cm and might approach 25 years of age (Bongrain, 1992). The extreme mineralization of their giant and heavy shells, observed also in other extinct species of Pliocene Pectinidae from North America and Japan (Ward and Blackwelder, 1975; Hayami and Hosoda, 1988), has no current equivalents in tropical-subtropical settings (Bongrain, 1988), and indicates high metabolic costs (Harzhauser et al., 2003).

P. jacobaeus is the largest scallop inhabiting the Mediterranean Sea today and can attain a shell length of up to 14–16 cm, and a maximum recorded age of 13 years (Peharda et al., 2003). This stenohaline species lives at depths ranging from 25 to 250 m, on sand, mud and gravel substrates, although is more common up to a depths <80 m (Poppe and Goto, 2000). *P. jacobaeus* first appeared in the Zanclean of the Mediterranean Sea (Monegatti and Raffi, 2001). In the Zanclean of southern Spain, it is common in assemblages from coarse-grained lithofacies, from siliciclastic and carbonate conglomerates to coarse and medium sands (Aguirre et al., 1996), where it often co-occurs with *G. latissimus* (e.g. García-Ramos and Zuschin, 2019). Present occurrences of *P. jacobaeus* are mostly registered in the Mediterranean Sea, with occasional reports from the Atlantic (e.g. Borges et al., 2010). It is closely related to *Pecten maximus*, which lives today in the eastern Atlantic, from Norway to Morocco, although it can also be found in the Mediterranean along the Alboran Sea coasts (Saavedra and Peña, 2005; Gofas et al., 2017). The two species can be easily distinguished by their shell morphology. However, genetic studies carried out with different types of markers indicate that *P. jacobaeus* and *P. maximus* could be morphs or subspecies (Wilding et al., 1999; Saavedra and Peña, 2004, 2005; Morvezen et al., 2016). Palaeontological evidence suggests that the common ancestor of the two was *Pecten grayi* Michelotti, 1839, which lived in the proto-Mediterranean Sea during the late Miocene (Fatton, 1973). The latter gave rise directly to *P. jacobaeus*, and indirectly, in the Pleistocene, to *P. maximus* via the Pliocene Atlantic species *P. grandis* (see Waller, 1991).

3. Material and methods

Studied specimens are two articulated valves of *G. latissimus* (GL1: length: 13.5 cm, height: 13.1 cm; GL2: length: 15.9 cm, height: 15.4 cm), two articulated valves of *P. jacobaeus* (PJ1: length: 11.3 cm, height: 9.4 cm; PJ2: length: 9.9 cm, height: 8.2 cm), and one partial left valve of *P. jacobaeus* (PJ3) (Fig. 2, S1b). All, except PJ3, were collected by Marino Tommasi, and donated to the Museo di Storia Naturale, University of Florence (Italy) by his heirs. Labels included information on the locality of origin added by Massimiliano Ghinassi at the donation (2014, personal communication). Museum catalogue numbers are: GL1: IGF 105164, GL2: IGF 105163; PJ1: IGF 105165; PJ2: IGF 105166; PJ3: IGF 105167 (IGF, Istituto Geologico Fiorentino).

Complete, well-preserved specimens, with the entire shell preserved, of the two species here under study are in general difficult to find. Moreover, the partially destructive approach undertaken (see below) does not warrant the use of historical museum collections. We proceed with the analysis of a small number of specimens, knowing that a larger number would have allowed to better characterise species adaptation to changing climate and environmental conditions.

3.1. Dating techniques

To better constrain the age of the studied outcrop, a biostratigraphic analysis of the sediment through calcareous nannofossils was performed, accompanied by Sr isotope analysis of the shells.

A sample of sediment was collected from the valves of PJ1 and examined for its calcareous nannofossil content. The sample was prepared as a smear slide following the standard preparation technique of Monechi and Thierstein (1985) and analysed using a polarizing microscope at 1250× magnification. The biostratigraphic investigation was conducted following the zonations of Backman et al. (2012), Okada and Bukry (1980) and Martini (1971).

Two small fragments of shell of GL1 and PJ1 were analysed for their elemental and isotopic Sr content. Sample preparation was performed in the Clean Room of the Filippo Olmi Laboratory of the Department of Earth Sciences of the University of Florence (Italy). Small chips of each sample were digested in PFA Savillex beakers using 7 M HNO_3. Chromatographic separation using Eichrom Sr-Spec resin was performed to ensure Sr purification from the matrix elements (following Avanzinelli et al., 2005). The collected fraction was then refluxed at 150 °C twice with concentrated HNO_3 and H_2O_2 to ensure the removal of any organic residue from the resin. About 200 ng of Sr in nitrate form was loaded onto a single Re filament along with $TaCl_5$ and H_3PO_4 to improve the ionisation efficiency and keep the stability of the signal during measurement. The isotopic composition of the two samples was analysed by Thermal Ionisation Mass Spectrometry (TIMS, Triton Plus, Thermo Fisher) in static mode, and is given as the average of 240 measurements for each sample. The instrumental mass bias was corrected off-line applying the exponential fractionation law to the measured $^{88}Sr/^{86}Sr$ ratio and the natural value ($^{88}Sr/^{86}Sr_N = 8.375209$). The isotope composition of the international reference standard NIST SRM987 analysed along with the samples was within the error of the long-term reproducibility, i.e., 0.710248 ± 0.000050 (2 s.d., $n = 148$), and in agreement with the values reported in Thirlwall (1991). The obtained $^{87}Sr/^{86}Sr$ values were converted into numerical ages using the regression curve LOESS look-up Table version 6 from McArthur et al. (2020) (Table S1).

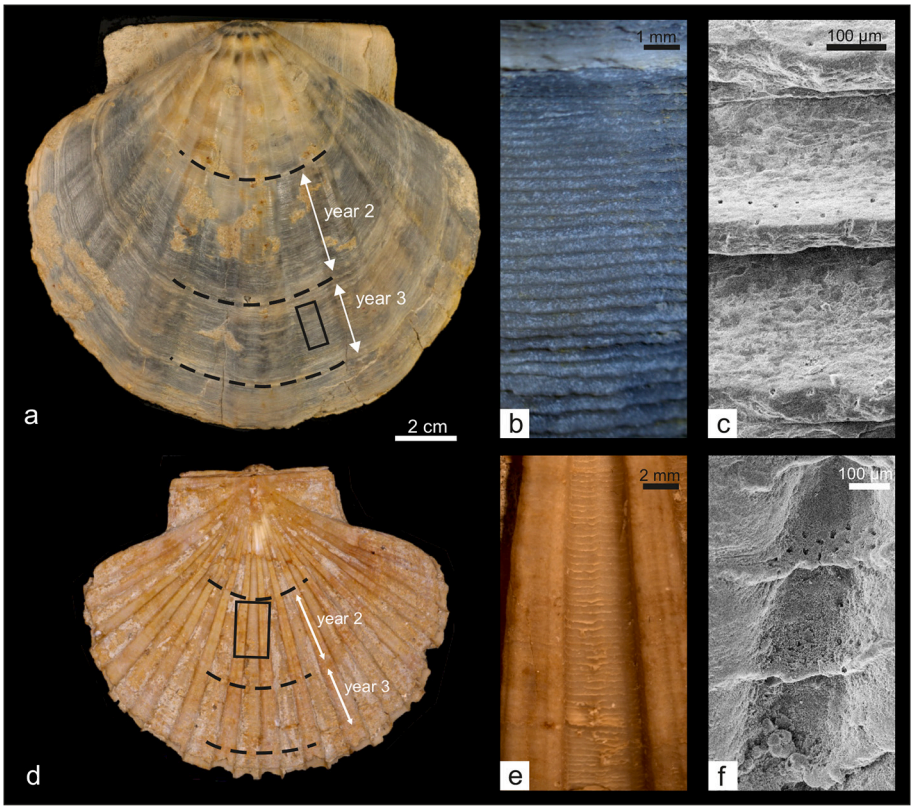

Fig. 2. Two of the studied specimens showing the annual growth lines and daily growth increments. (a) *G. latissimus* (specimen GL1). (b) Enlargement of the boxed area indicated in (a), showing detail of the micro-growth increments. (c) SEM image showing the microstructure of micro-growth increments in *G. latissimus*, which are pierced by numerous small holes. (d) *P. jacobaeus* (specimen PJ1). (e) Enlargement of the boxed area indicated in (d), showing detail of the micro-growth increments. (f) SEM image showing the microstructure of -micro-growth increments in *P. jacobaeus*, which are pierced by numerous small holes. Small planktonic foraminifera at the bottom. Black dashed lines in (a) and (d) indicate annual rings. White arrows indicate years 2 and 3 on the shell surface.

3.2. Shell preservation

The degree of preservation of the original calcite (e.g. possible presence of neomorphic minerals and the ultrastructure of the outer layer) of the five specimens was assessed using a scanning electron microscope (SEM, Fig. S2), and by minor and trace element analysis (Mn, Fe, Sr: Table S2).

For SEM analysis small shell fragments (1–2 cm in size) were removed from right valves. The surface of the samples was etched with 5% *v*/v hydrochloric acid for 5–10 s to reveal the microstructure before rinsing with deionized water. Dry specimens were then gold-coated with a Quorum Q150R ES, and studied with a ZEISS EVO MA15, equipped with an Everhart–Thornley detector, at the M.E.M.A laboratory of the University of Florence (Italy). Samples were observed in secondary electron signal at 48× to 4× magnification.

For elemental analyses (Mn, Fe and Sr), powder samples were collected close to the transect of isotope sampling where the shell looked pristine, and in areas where shells looked altered (e.g. orange stains). Around 30 mg of powder for each sample was totally digested with 1 ml 7 M HNO_3 and measured at the University of Florence using an ICPMS (Agilent 7800) using Rh as internal standard and a multi-elemental standard solution for calibration (Inorganic Ventures, VA, USA). Accuracy and precision were tested by replicate measurements of the certified rock standards AGV-1 (andesite) and JLs-1 (limestone) (see Table S2). AGV-1 standard yielded results within 1% of the refence values (GeoRem database: Jochum et al., 2005); JLs-1 measurements provided values within the range of previously published ones (GeoRem database: Jochum et al., 2005) that are however more variable.

3.3. Growth increment widths

Width of micro-growth increments was measured on the surface of the left shell along the axis of maximum growth. When possible, measurements were taken from the second and third annual cycles (GL1, GL2, PJ1), which were identified by counting prominent visible marks on the surface of shells, interpreted as annual in modern Pectinidae ("annual rings"; e.g. Mason, 1957; Roux et al., 1990; Schein et al., 1991; Barbin et al., 1991; Chauvaud et al., 2012; Peharda et al., 2019). The first years of growth were chosen in order to measure parts of the shell with fastest seasonal growth, as growth rate decreases during the lifespan of bivalves (e.g. Goodwin et al., 2003). On PJ2, prominent annual rings were not visible, and growth increment widths were measured on a part of the shell from which sediment had been removed (total of 3.2 cm, Fig. S1b). On PJ3, that is only partially preserved (Fig. S1b), we sampled what we considered a full annual cycle, which we tentatively interpreted as the second year of growth. Micro-growth increments were measured at µm-resolution (error 0.7%) on digital images taken with a Zeiss Stemi 508 binocular microscope equipped with a 5 megapixel 5MP HDMI Oculux CAM digital camera, with dedicated software for image analysis called Image View. To compare relative differences in shell growth, widths of micro-growth increments of the five specimens have been normalised to the largest measured value.

3.4. Stable carbon and oxygen analysis

Before sampling for $\delta^{13}C$ and $\delta^{18}O$ values, specimens were cleaned by brushing them under deionized water to remove the surrounding matrix, mostly made of silt and fine sand. To better remove the matrix and the small foraminifera trapped between lamellae, the valves of

P. jacobaeus were additionally immersed in an ultrasonic bath with deionized water for 30 min each, and then rinsed in deionized water. After drying the valves in an oven at 40 °C, powder samples were collected by milling small sample swaths from the shells by hand under a stereo microscope using a DREMEL 3000 equipped with a Komet (Komet-Brasseler GmbH & Co. KG) drill bit. The drill bit is made of tungsten carbide, its tip has a diameter of 300 μm with rounded burs (model H71 104,003). Milling was completed parallel to the growth striae, avoiding parts of the shell still covered by matrix. Average swath length is 2500 μm for *P. jacobaeus* and 4580 μm for *G. latissimus*; average width is 425 μm for *P. jacobaeus* and 380 μm for *G. latissimus*, depth is around half of width. In total, 304 samples for stable isotopes were collected: 55 from GL1 (27 from year 2; 28 from year 3), 79 from GL2 (51 from year 2; 28 from year 3), 35 from PJ1 (18 from year 2; 17 from year 3), 58 from PJ2 (no information on year), 27 from PJ3 (7 from year 1?; 20 from year 2?).

Carbonate samples of ca. 100 μg of $CaCO_3$ were dissolved in H_3PO_4 (100%) for 1 h at 70 °C and mass spectrometric measurements were made on evolved CO_2 gas using a Gas Bench II (Thermo Scientific) coupled to a Delta Plus (Finnigan MAT) at the "Stable Isotopes Laboratory" of the Institute of Geosciences and Earth Resources of the Italian National Research Council (IGG-CNR), Pisa (Italy). All sample were measured twice. In this work, results are reported relative to the Vienna Pee Dee Belemnite (VPDB). Calibration of the data was accomplished with a three-point calibration using in-house standards MS ($\delta^{13}C$ = 2.13‰, $\delta^{18}O$ = −1.73‰), MOM ($\delta^{13}C$ = 2.53‰ $\delta^{18}O$ = −4.73‰) and NEW12 ($\delta^{13}C$ = −3.83‰, $\delta^{18}O$ = −9.59‰), previously analysed by external research laboratories. NBS-18 was used for internal quality check. The mean analytical precision, calculated considering 1 STDEV for repeated MS standard (n = 40), was ±0.09‰ for $\delta^{13}C$ and ± 0.12‰ for $\delta^{18}O$.

After linearly interpolating micro-growth increment widths and $\delta^{13}C_{shell}$ and $\delta^{18}O_{shell}$ values, in order to have equally spaced values (regular interpolation function, software Past), cross plots of normalised micro-growth increment widths versus $\delta^{13}C_{shell}$ and $\delta^{18}O_{shell}$ values were created, to compare the relative growth of the two species at given values of $\delta^{13}C$ and $\delta^{18}O$. After that, the Pearson correlation coefficient (r) and the coefficient of determination (r^2) were calculated, applying the Bonferroni correction on the p value.

3.5. Estimate of palaeotemperature

The isotopic composition of the shell of bivalves can be used as a proxy for temperature and the oxygen isotope signature (and salinity) of the ambient water during biomineralization, as most bivalves form their shells in oxygen isotope equilibrium with the ambient aquatic medium, and seasonally changing seawater temperatures (and salinity) affect $\delta^{18}O_{shell}$ values (Jones et al., 1989; Wefer and Berger, 1991; Weidman and Jones, 1994; Surge et al., 2001; Ivany et al., 2008; Schöne and Surge, 2012). A shift in $\delta^{18}O_{shell}$ towards more positive values indicates colder temperatures, whereas more negative values reflect warmer temperatures.

Many equations have been developed over the years to estimate palaeotemperatures from $\delta^{18}O_{shell}$. Here we used the equation of Anderson and Arthur (1983), one of the most frequently used in palaeoclimatic studies (e.g. Bice et al., 1996; Immenhauser et al., 2005; Lartaud et al., 2010; Walliser et al., 2016; Briard et al., 2020; see also Wierzbowski, 2021 for a comparison of different equations), for low Mg-calcite bivalves:

$$T(^{\circ}C) = 16.0–4.14^{*}\left(\delta^{18}O_{shell} - \delta^{18}O_{sw}\right) + 0.13^{*}\left(\delta^{18}O_{shell} - \delta^{18}O_{sw}\right)^2$$

where T is the water temperature in °C, $\delta^{18}O_{shell}$ is the $\delta^{18}O$ value of the sample and $\delta^{18}O_{sw}$ the $\delta^{18}O$ value of seawater. $\delta^{18}O_{shell}$ and $\delta^{18}O_{sw}$ values are expressed relative to VPDB and VSMOW, respectively.

Estimating the value of $\delta^{18}O_{sw}$ correctly is fundamental to obtain accurate palaeotemperature reconstructions. The local or regional $\delta^{18}O_{sw}$ value is a function of the global mean seawater composition as well as geographical variations caused by the combined effects of changes in evaporation/precipitation patterns, runoff (in coastal regions), and ocean circulation patterns (Zachos et al., 1994; Schmidt, 1998). As there are no direct data for the oxygen stable isotope composition of seawater in the mid-Pliocene of the Mediterranean area, the value of $\delta^{18}O_{sw}$ has been assumed taking into consideration reconstructions of the climate regime of this time interval and model simulations.

The current Mediterranean hydrological cycle is unbalanced. The mean annual precipitation, about 400 mm/yr, and the mean annual runoff, about 100 mm/yr, do not compensate for the large evaporation rates occurring over the Mediterranean Sea (≈1000 mm/yr), resulting in a deficit in the hydrological budget (Mariotti et al., 2002). Depending on studies, current values of $\delta^{18}O_{sw}$ of surface waters are 0.76–1.37‰ (Pierre, 1999) or 0.13–2.29‰ (Dämmer et al., 2020) in the western, and 1.30–1.66 ‰ (Pierre, 1999) or 0.73–2.43‰ (Dämmer et al., 2020) in the eastern Mediterranean Sea, with a general increase towards the north and towards the east, which mirrors an increase in salinity (Pierre, 1999). Estimates from the modern Tyrrhenian Sea are 1.00–1.33‰ (Iacumin et al., 1992; Pierre, 1999).

Pollen and macroflora remains from several sites of the peri-Mediterranean region, together with climate models for the Mediterranean area, indicate that the late Zanclean-Piacenzian interval was characterized by relatively stable climatic conditions, with a humid climate, values of temperature and humidity higher than today, and lower seasonality (e.g. 1–5 °C warmer and 400–1000 mm/yr wetter than present: Haywood et al., 2000; Fauquette et al., 2007; Jost et al., 2009). High precipitation was, however, balanced by high evaporation rates, which are estimated about 50% larger than pre-industrial levels (Colleoni et al., 2015; Tindall and Haywood, 2015). According to the climate model of Tindall and Haywood (2015), the $\delta^{18}O_{sw}$ value of the Mediterranean Sea was slightly more positive than today, with average values ranging from 1 to 1.5‰, due to a more intense hydrological cycle and higher salinity. Ragaini et al. (2019) estimated that $\delta^{18}O_{sw}$ values would have been around 0.25‰ lower than now, i.e., about 0.9‰ in the western Mediterranean during the mid-Pliocene. They used this value in reconstructing paleotemperatures from a shell of the venerid bivalve *Pelecyora gigas* from the Siena-Radicofani basin. In the absence of tighter constraints, we chose to estimate palaeotemperature using the two available extremes, 0.9‰ as estimated by Ragaini et al. (2019), and 1.5‰ as the maximum value of Tindall and Haywood (2015).

4. Results

4.1. Age of the samples

Following biostratigraphic analysis, we observed a Pliocene calcareous nannofossil assemblage characterized by common and moderately to well preserved coccoliths. Moderately preserved specimens, despite the evidence of etching and/or overgrowth in the primary morphological characters, do not prevent identification at the species level. The assemblage consists of abundant small *Gephyrocapsa* spp., common *Coccolithus pelagicus*, occasional *Pontosphaera* spp., *Reticulofenestra minutula* (5–6 μm) and rare *Discoaster* in the form of *D. asymmetricus, D. brouweri, D. surculus* and *D. tamalis*. Other rare species include *Braarudosphaera bigelowii, Calcidiscus leptoporus, C. macintyrei, Helicosphaera carteri and Pseudoemiliania lacunosa.* The occurrence of *D. tamalis, D. asymmetricus* and the absence of *R. pseudoumbilicus* (see also Fig. S3) enables us to identify the following biozones: the lower *D. tamalis* Top Zone (CNPL4) of Backman et al. (2012), CN12a of Okada and Bukry (1980) and NN16 of Martini (1971), spanning from the late Zanclean to Piacenzian. The assemblage is also characterized by Paleogene and Cretaceous reworked taxa in the form of occasional *Sphenolithus* spp. and rare *D. barbadiensis* and *Micrantolithus* sp. According to Backman et al.

(2012) the estimated age of the CNPL4 Zone is 3.81–2.76 Ma.

$^{87}Sr/^{86}Sr$ analyses gave the same mean ratios for the two analysed shells (GL1, PJ1) of 0.709061 (± 0.000007). These values, converted into numerical ages according to the calibration curve of McArthur et al. (2020), correspond to an average age range of 3.672–2.580 Ma (Table S1). As such, dates obtained from Sr isotope stratigraphy largely confirm biostratigraphic results, indicating a late Zanclean-Piacenzian age for the samples.

4.2. Bivalve preservation

In *P. jacobaeus* and in the closely related *P. maximus* the external surface of the outer layer is organized in thin lamellae pierced by numerous small holes (cribriform lamelleae; Bongrain, 1988; Chauvaud et al., 2005). A similar cribiform structure of the outer layer is also present in *G. latissimus*, although the lamellae are wider than in *P. maximus*, and their inner part is characterized by small ovoidal bumps (see Bongrain, 1988: plate 1). This, and other similarities in the shell structure of *P. maximus* and species of the genus *Gigantopecten*, like the presence of a calcitic middle layer (see Taylor et al., 1969), point to a phylogenetic affinity between the two genera (Bongrain, 1988). The lamellae of the outer layer, with their cribiform structure, are preserved in the studied specimens, as shown by optical microscopy and SEM images (Fig. 2, Fig. S2). Furthermore, in specimens of *G. latissimus* and *P. jacobaeus*, the holes are empty (Fig. S2c, h), pointing to a good preservation of the outer shell layer that was sampled for oxygen and carbon stable isotope analyses.

The outer shell layer of Pectinidae is made of foliated low Mg-calcite (Taylor et al., 1969; Carter, 1990). Because of the stability of this mineralogical composition the shell is relatively immune to diagenetic processes like dissolution and recrystallization (see Marshall, 1992). An established tool to check the degree of calcite preservation, to be used in

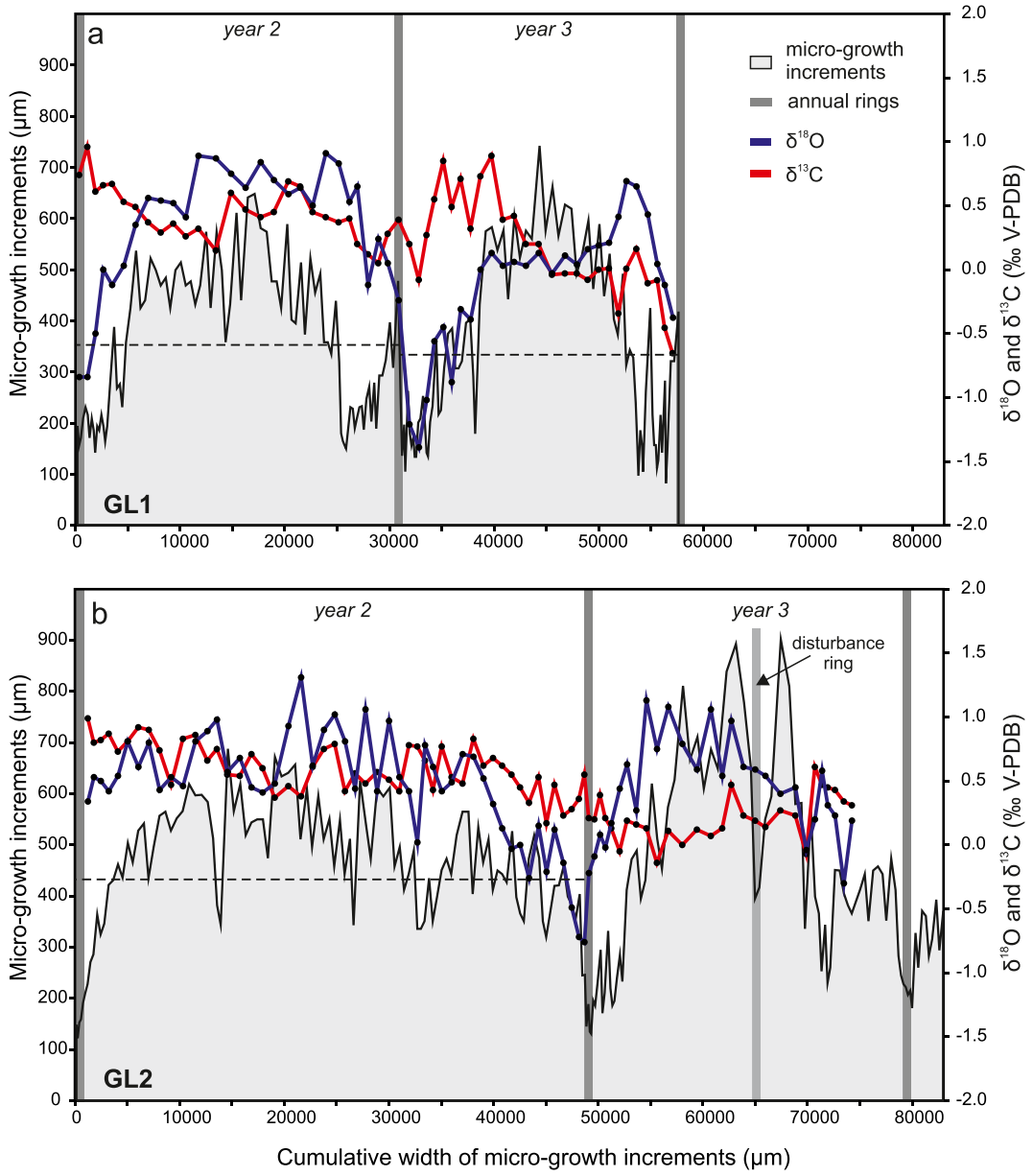

Fig. 3. Micro-growth increment widths and stable carbon and oxygen isotope data for *G. latissimus*. (a) Specimen GL1, second and third year of growth. (b) Specimen GL2, second and third year of growth. Dark-grey vertical bars indicate visible annual growth lines on the surface of the shell. Dotted, horizontal lines indicate the mean size of micro-growth increments in complete annual cycles (see Table 1). The distance between the dorsal margin and the point where we started measuring the width of micro-growth increments is 4.5 cm in GL1 and 5.5 cm in GL2.

combination with other screening techniques like optical and SEM imaging is the measurement of the concentration of minor (Sr) and trace elements (Fe, Mn) (Ullmann and Korte, 2015 and references therein). As meteoric water generally contains more Mn and Fe and less Sr compared with seawater, Fe and Mn concentrations increase and Sr concentration decreases in diagenetically altered marine carbonates (Brand and Veizer, 1980; Marshall, 1992). Mn and Fe composition of recent marine bivalves ranges between 1 and 250 p.p.m., and values of Sr between 700 and 1900 p.p.m. (Immenhauser et al., 2016). Mn concentrations of the studied specimens are all extremely low (between 14 and 43 p.p.m., Table S2), and Fe concentrations are all reasonably low (below 300 p.p.m.), except for one sample coming from an area of *G. latissimus* covered in orange stain (436 p.p.m.) that was avoided during isotopic sampling. Sr values are all above 700 p.p.m., except one (545 p.p.m., Table S2). In any case, a good preservation of the specimens is also supported by the positive correlation between Mn and Sr values (Table S2), in contrast to the negative correlation that is supposed to be characteristic of partially altered material (Ullmann and Korte, 2015).

4.3. Patterns of growth in Gigantopecten latissimus

In both specimens of *G. latissimus*, the width of micro-growth increments is highly variable, with minimum values of 100–200 μm and maximum values of 600–700 μm in GL1 and up to 900 μm in GL2 (Figs. 3, 5, Table S3). The narrowest micro-growth increments occur in the proximity of prominent growth lines on the outer shell surface (Figs. 2–3). In modern Pectinidae, these prominent growth lines, or annual rings, are interpreted to be formed annually, during periods of extremely slow accretion and/or cessations of bivalve growth (e.g. Chauvaud et al., 2005; Peharda et al., 2003). The widest micro-growth increments occur in the middle between annual rings, with intermediate width-values in-between, so that growth variation approximates a parabolic shape (Fig. 3). Two growth cycles are well recognizable both in GL1 and GL2 (Fig. 3). This general pattern has some exceptions, for instance in GL2, at around 65000 μm, there is an abrupt decrease in the micro-growth increment width, followed by a sudden increase, forming a prominent line on the shell surface (Fig. 3). We counted 81 micro-increments in the second year of growth and 66 in the third year for GL1; 121 in the second year and 69 in the third year for GL2 (Table 1). The average width of the micro-growth increments is 341 μm in GL1 and 434 μm in GL2; GL2 has overall higher width of increments compared to GL1 (Table 1, Fig. 6). GL2 also attained a larger size (length 15.9 cm, height 15.4 cm) compared to GL1 (length 13.5 cm, height 13.1 cm).

Resolution of $\delta^{18}O_{shell}$ and $\delta^{13}C_{shell}$ curves is lower compared to the micro-growth increment curves, as powder samples were obtained from 1 to 4 micro-growth increments, depending on the width of the increments. Notwithstanding this, it is possible to observe that, overall, the shape of the oxygen isotope curve shows a similar pattern to that of the micro-growth increment widths: high $\delta^{18}O_{shell}$ values correspond to wider growth increments and low $\delta^{18}O_{shell}$ values to narrower growth increments (Fig. 3). This positive correlation is also observed when, after linear interpolation, normalised growth increment widths are plotted against $\delta^{18}O_{shell}$ values (Fig. 5a; r: 0.43 in GL1 and r: 0.47 in GL2). Despite this, $\delta^{18}O_{shell}$ values only partially explain the variation of micro-growth increments width (r^2: 0.19; p: 0.001 in GL1; r^2: 0.22; p: <0.0001 in GL2). In fact, although the positive correlation is broadly valid, there are some parts of the shells where $\delta^{18}O_{shell}$ values are high and micro-growth increment width is low (towards the end of years 2 and 3 in GL1) or $\delta^{18}O_{shell}$ values are falling and micro-growth increment width is rising (middle part of year 3 in GL2). Correlation between $\delta^{13}C_{shell}$ values and micro-growth increment widths is slightly negative and $\delta^{13}C_{shell}$ values do not explain variation in shell growth (r: −0.05; r^2: 0.002; p: 0.70 in GL1; r: −0.22; r^2: 0.05; p: 0.05 in GL2; Fig. 5b). Despite this, in GL1 low micro-increment width mostly coincides with intervals of high $\delta^{13}C_{shell}$ values, and this is observed especially at the beginning of each annual' cycle (Fig. 3a). This can be also observed at the beginning of the second annual cycle of GL2 (Fig. 3b). In both specimens, $\delta^{18}O_{shell}$ and $\delta^{13}C_{shell}$ curves are not correlated (Fig. S6). GL1 $\delta^{18}O_{shell}$ and $\delta^{13}C_{shell}$ values are slightly lower than those of GL2 (Fig. 7a-b).

Table 1
Width of micro-growth increments for each measurable annual cycle.

	GL1	GL1	GL2	GL2	PJ1	PJ1	PJ3
	year 2	year 3	year 2	year 3	year 2	year 3	year 2?
No.	81	88	121	69	74	73	97
min size	142	82	122	181	82	97	45
max size	648	742	688	902	537	486	463
avg size	352.5	332.0	426.0	451.9	277.6	256.8	236.2

4.4. Patterns of growth in Pecten jacobaeus

In *P. jacobaeus* the shape of the curves of the micro-growth increment widths is less regular compared to *G. latissimus*, and prominent growth lines, attributable to slow growth and low biomineralization rate, are less visible (Figs. 2, 4b, Fig. S2). The second annual cycle of PJ1 is incomplete during the first half of the main growing season, while the third year, which is complete, displays a more regular curve, with narrow micro-growth increments at the two sides, and wide increments in the middle part (Fig. 4a). In the last part of the second year, micro-growth increments were so closely spaced that it was impossible to measure their width (straight line in micro-growth increments at 20000-24000 μm from the dorsal margin, Fig. 4a). In PJ2, where prominent growth lines were not observed (Fig. S2), it is hard to find a cyclicity in the growth patterns. Growth increments are narrow in the first measured part, up to 14000 μm from the dorsal margin (Fig. 4b), and then remain of medium or high width until the end of the sampled transect (Fig. 4b). PJ3 shows more regular growth patterns, with narrow micro-growth increments before the first observed annual ring, wide increments in the following annual cycle, which could correspond to the second year of growth, and decreasing micro-growth increment width towards the end (Fig. 4c). In PJ1, we counted 74 micro-growth increments in the second year, although this number is underestimated as in the interval between 20.000 and 25.000 μm the lamellae were so closely spaced that it was impossible to count and measure them, and 73 in the third year (Table 1, Fig. 4a). In PJ3 we counted a total of 97 micro-growth increments in what could be the second year. The average width of the micro-growth increments is 267.7 μm in PJ1, 212.6 in PJ2 and 202.5 in PJ3. PJ1 has wider micro-growth increments compared to PJ2 and PJ3 (Table 1, Fig. 6a). PJ2 also reaches a maximum size (width 9.9 cm, height 8.2) smaller than PJ1 (length 11.3 cm, height 9.4 cm). Micro-growth increments of *P. jacobaeus* tend to be narrower than those of *G. latissimus*: the largest micro-growth increments of *P. jacobaeus* are included in the third quartile of the size-distribution of *G. latissimus* (Fig. 6).

For *P. jacobaeus*, samples for $\delta^{18}O_{shell}$ and $\delta^{13}C_{shell}$ analyses were collected from 1 to 6 micro-growth increments, apart from one part of PJ3 where micro-growth increments were so closely spaced that one sample covers 25 increments (Fig. S1b). Because of the narrower size of the micro-growth increments of *P. jacobaeus* compared to *G. latissimus*, sampling resolution is lower in the former. In PJ1, a decrease in width of micro-growth increments during year 2 is coupled with a decrease in $\delta^{18}O_{shell}$ values; in year 3, the shape of the $\delta^{18}O_{shell}$ curve resembles that of the micro-growth increment widths (Fig. 4a). The correlation between the interpolated growth increment widths and $\delta^{18}O_{shell}$ is positive (r: 0.30) although oxygen isotope data do not explain in a significant way the variation of micro-growth increments (r^2: 0.09; p: 0.08; Fig. 5c). In PJ3 there is also a positive correlation between $\delta^{18}O_{shell}$ and growth increments, which is significant (r: 0.5; r^2: 0.25; p: 0.007; Figs. 4c, 5c). In PJ2, narrow micro-growth increments correspond to high $\delta^{18}O_{shell}$ values, and vice versa (Fig. 4b). The correlation of the interpolated data between $\delta^{18}O_{shell}$ and growth increment widths is negative, although

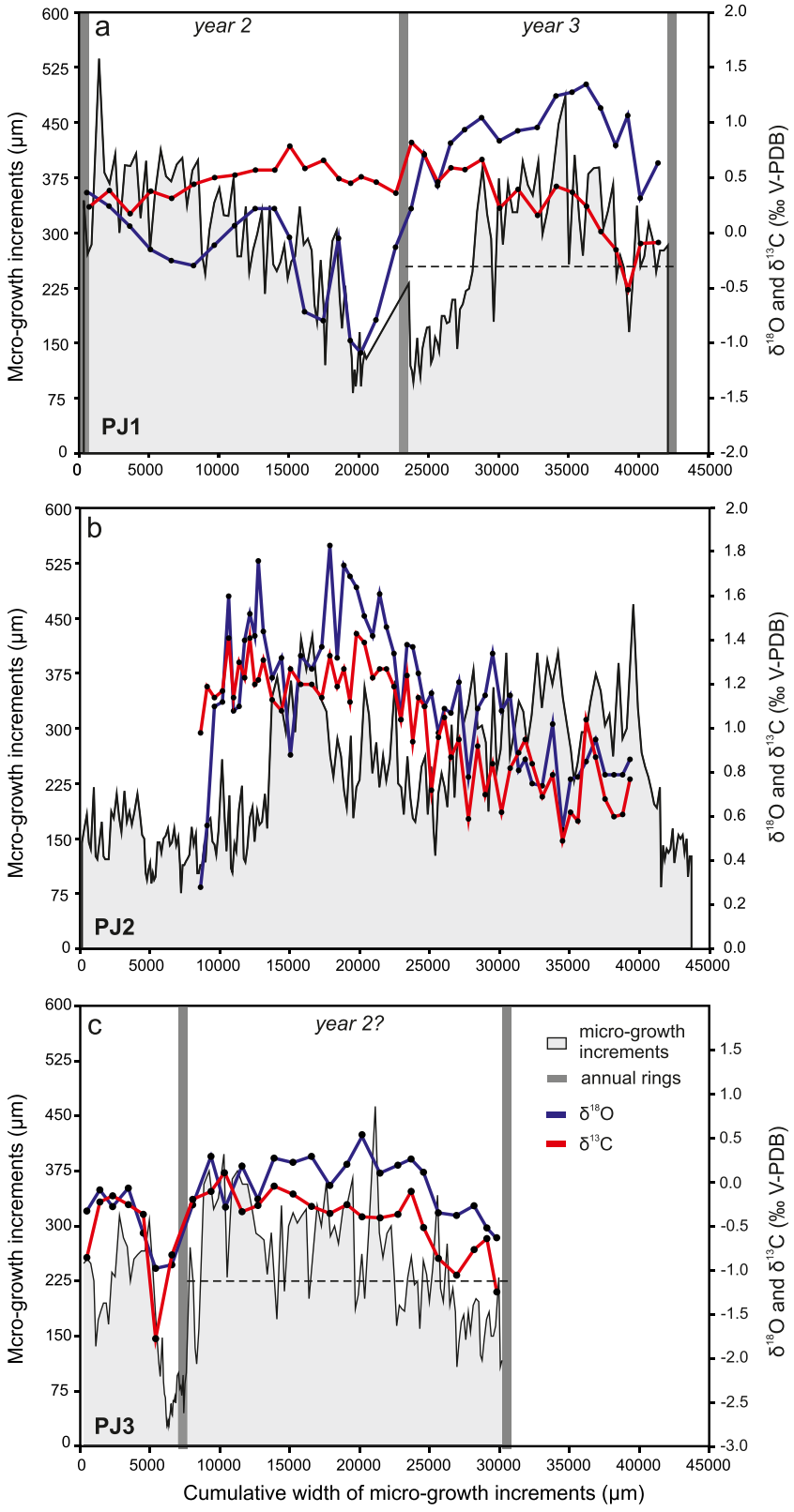

Fig. 4. Micro-growth increment widths and stable carbon and oxygen isotope data for *P. jacobaeus.* (a) Specimen PJ1, second and third year of growth. (b) Specimen PJ2, no annual growth lines visible on the surface of the shell. (c) Specimen PJ3, second? year of growth. Dark-grey vertical bars indicate visible annual growth lines on the surface of the shell. Dotted, horizontal lines indicate the mean size of micro-growth increments in complete annual cycles (see Table 1). The distance between the dorsal margin and the point where we started measuring the width of micro-growth increments is 3.76 cm in PJ1 and 1.98 cm in PJ2; the same measurement cannot be taken on PJ3 because the specimen is broken.

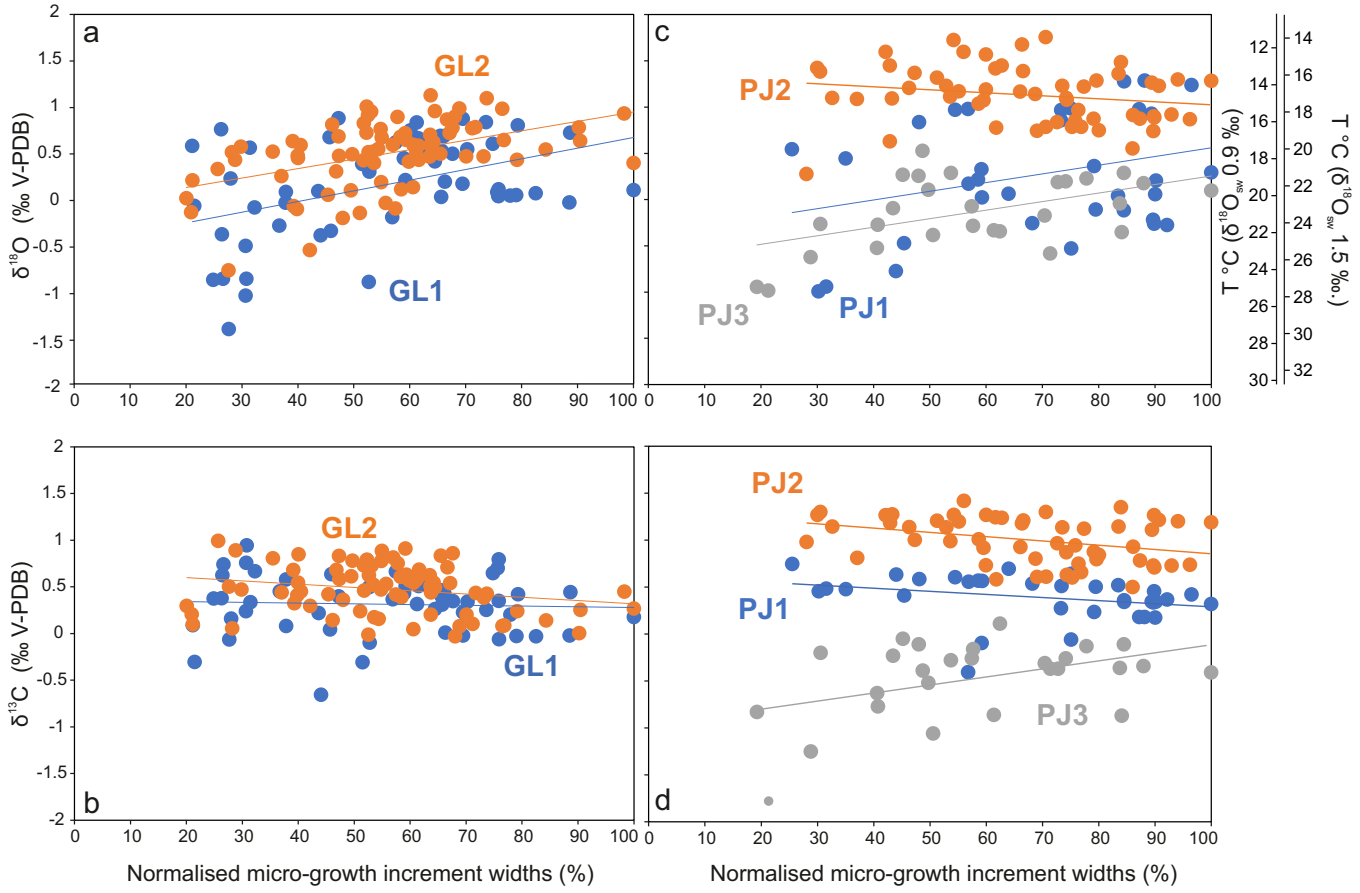

Fig. 5. Cross plots of normalised, linearly interpolated micro-growth increment widths and oxygen and carbon stable isotope values. (a) GL1 (r: 0.43; r^2: 0.19; p: 0.001) and GL2 (r: 0.47; r^2: 0.22; p: <0.0001) normalised growth increment widths versus $\delta^{18}O_{shell}$ values. (b) GL1 (r: −0.05; r^2: 0.002; p: 0.70) and GL2 (r: −0.22; r^2: 0.05; p: 0.05) normalised growth increment widths versus $\delta^{13}C_{shell}$ values. (c) PJ1 (r: 0.30; r^2: 0.09; p: 0.08), PJ2 (r: −0.19; r^2: 0.04; p: 0.15), PJ3 (r: 0.50; r^2: 0.25; p: 0.007) normalised growth increment widths versus $\delta^{18}O_{shell}$ values. (d) PJ1 (r: −0.29; r^2: 0.08; p: 0.09), PJ2 (r: −0.35; r^2: 0.12; p: 0.008), and PJ3 (r: 0.43; r^2: 0.19; p: 0.02) normalised growth increment widths versus $\delta^{13}C_{shell}$ values. Lines are linear regression curves. After Bonferroni correction, r^2 are significant at $p < 0.025$.

oxygen isotope data do not significatively explain the variation of growth increment widths (r: −0.19; r^2: 0.04; p: 0.15; Fig. 5c). In PJ1, $\delta^{13}C_{shell}$ values do not show a strong variability, and are negatively correlated with the growth-increment curve (Figs. 4a, 5d). There is in PJ2 also a negative correlation, but this is significant (Fig. 5d). In PJ3, on the other hand, there is a positive correlation between interpolated growth-increments and $\delta^{13}C_{shell}$ (Fig. 5d). The correlation between $\delta^{18}O_{shell}$ and $\delta^{13}C_{shell}$ is positive and significant for PJ2 (r: 0.68; r^2: 0.47; $p < 0.0001$) and PJ3 (r: 0.67; r^2: 0.45 p: 0.0001), and negative, although not significant in PJ1 (r: −0.35; r^2: 0.1; p: 0.04; Fig. S10). In terms of absolute values, $\delta^{18}O_{shell}$ and $\delta^{13}C_{shell}$ values of PJ1 are in the same range of variation as GL1 and GL2, as PJ1 interquartile range includes the interquartile range of GL1 and GL2 (Fig. 7). PJ2 has higher values for both parameters compared to PJ1, GL1 and GL2. $\delta^{18}O_{shell}$ values of PJ3 are included within the median and the minimum scores of the first three shells, while $\delta^{13}C_{shell}$ values are mostly lower than those of the other shells (Fig. 7).

4.5. Seasonal palaeotemperatures

Palaeotemperature estimates are >2 °C higher applying a value of $\delta^{18}O_{sw}$ of 1.5‰ compared to estimates using a value of 0.9‰ (Figs. 7, 8, Table S4). Overall, GL1, GL2, PJ1 and PJ3 record similar ranges of palaeotemperatures, but PJ2 shows lower values (Figs. 7, 8). The interquartile ranges of GL1, GL2, PJ1 and PJ3 estimated for $\delta^{18}O_{sw=0.9}$, are all between 16 and 21 °C, but the interquartile range of PJ2 is colder (14–16 °C), with almost no overlap with the other four specimens (Fig. 7). The coldest temperature, recorded by PJ2, is 12 °C for $\delta^{18}O_{sw=0.9}$ and 14.8 °C for $\delta^{18}O_{sw=1.5}$ (Figs. 7, 8). The highest temperature is registered by GL1: it is 26 °C for $\delta^{18}O_{sw=0.9}$ and 29 °C for $\delta^{18}O_{sw=1.5}$. The coldest temperature, excluding the values of PJ2, is equally registered by GL2 and PJ1, and is 14 °C for $\delta^{18}O_{sw=0.9}$ and 16.8 °C for $\delta^{18}O_{sw=1.5}$ (Figs. 7, 8).

For both species, except for PJ2, micro-increment width is lower when temperature is higher (in summer; Fig. 5c). Maximum temperature is registered just before (PJ1, PJ3) or after (GL1) the growth break, except in GL2, where the maximum temperature coincides with it (Fig. 8). Therefore, PJ1, PJ3 and GL1 most likely register both minimum winter temperature and peak summer temperature.

5. Discussion

5.1. Seasonal growth-strategy of Pliocene G. latissimus and P. jacobaeus

Prominent growth lines, or rings, found on the surface of the shell of Pectinidae, as on other bivalves, are usually interpreted to be formed with an annual periodicity, and to represent annual periods of growth slowdown and eventually cessation (Clark II, 1974; Richardson, 2001; Chauvaud et al., 2005; Louis et al., 2022). However, large, non-periodic growth lines can also be formed due to environmental disturbances (e.g. storms) and biological (e.g. reproduction and predation) factors (Goewert and Surge, 2008; Schöne, 2008). The study of micro-growth patterns can enhance our understanding of factors controlling bivalve growth. For instance, any abrupt decrease in micro-growth increment

widths over short time scales, related perhaps to disturbance or spawning, can be distinguished from the gradual changes in increment widths associated with seasonal growth patterns (Owen et al., 2002a). This has also been observed in modern *P. jacobaeus,* where disturbance rings are characterized by nearly equally spaced lamellae immediately before and after the environmental disturbance, whereas annual rings are associated with small, crowded lamellae (Peharda et al., 2003). Furthermore, while for modern specimens direct monitoring of environmental and growth conditions can help to distinguish between periodic annual and non-periodic growth patterns, in fossil specimens the combination of growth patterns and geochemical data can help in identifying seasonal growth patterns (Jones and Allmon, 1995; Williams et al., 2010; Johnson et al., 2019).

In our study, the regular, bell-shaped pattern of micro-growth increment widths observed in the two specimens of *G. latissimus*, which are delimited by distinct growth lines associated with very low growth rates, indicates that shell growth follows an annual periodicity (Fig. 3). The presence of annual growth patterns in specimens of *G. latissimus* is supported by the seasonal cycle shown by $\delta^{18}O_{shell}$ data, with minimum values concomitant with narrow micro-growth increments and annual growth lines, and maximum values associated with wide micro-growth increments (Fig. 3). This indicates that *G. latissimus* formed its shell mainly during the colder months, and that growth slowdown occurred during the warmer season, as shown by the "rounded" winter and more cuspate summer sectors of the $^{18}O_{shell}$ profiles. Also the positive correlation between the width of micro-growth increments and $\delta^{18}O_{shell}$, observed in both studied specimens, suggests that growth was probably faster during winter compared to summer (Fig. 5a). Abrupt decreases in the width of growth- increments followed by an equally rapid increase, are sometimes observed (e.g. GL2 at around 65000 μm from the shell dorsal margin, Fig. 3b), and are interpreted instead as disturbance rings.

Overall, PJ1 and PJ3 show seasonal growth patterns similar to those of *G. latissimus*, with faster growth at colder temperatures and slower growth at higher temperature (Figs. 4, 8). Indeed, also, in PJ1 and PJ3 there is a positive correlation between the width of micro-growth increments and $\delta^{18}O_{shell}$ values (Fig. 5c). The same relationship between prominent growth lines observed on the external shell surface and seasonal $\delta^{18}O_{shell}$ cycles has been observed in modern *Pecten jacobaeus* from the Northern Adriatic Sea (Peharda et al., 2019). In these specimens, collected at depths between 25 and 30 m along the western coast of the Istrian peninsula, major growth lines coincided with $\delta^{18}O_{shell}$ minima, suggesting that growth slowdown and potentially cessation occurred during the warmest part of the year. By contrast, highest $\delta^{18}O_{shell}$ values (corresponding to lowest water temperature) were detected in fastest-growing shell portions of the growing season (Peharda et al., 2019). Furthermore, no, or very little shell growth occurred during a period of approximately five months, between July and November, while shells grew at fastest rates during winter and spring (Peharda et al., 2019). This information suggests that, at least two of the three studied fossil specimens of *P. jacobaeus* had a growth-behaviour similar to modern specimens, characterized by summer growth slow down and/or cessation.

PJ2 differs from the other studied specimens for two main reasons. First, there are no prominent growth lines on the surface of the shell (Fig. S1b); second, it is not possible to identify a clear seasonal cyclicity by comparing the trend of micro-growth increment widths and oxygen isotope values (Fig. 4b). Also $\delta^{18}O_{shell}$ values do not significantly explain variation in growth (Fig. 5c). The absence of prominent growth lines on the surface of Pectinidae is not untypical, especially in the juvenile part of the shells (Owen et al., 2002a), which we have sampled. Furthermore, the absence of a clear cyclic signal in $\delta^{18}O_{shell}$ values might be indicative of calcification under less seasonal conditions, for instance, at a high depth below the mixed layer (e.g. Johnson et al., 2000; Johnson et al., 2021a, 2021b; Chauvaud et al., 2011). The high, positive correlation between $\delta^{18}O_{shell}$ and $\delta^{13}C_{shell}$ supports this interpretation, because bivalves that live above the thermocline sometimes show a negative covariation between $\delta^{18}O_{shell}$ and $\delta^{13}C_{shell}$ values (i.e., antiphase ontogenetic profiles), while bivalves living below it show a positive covariation (i.e. in-phase ontogenetic profiles; Arthur et al., 1983). Theoretically, if $\delta^{13}C_{shell}$ values in shallow water bivalves were only controlled by variations of the $\delta^{13}C$ of dissolved inorganic carbon (DIC), excluding the role of metabolic and kinetic effects (see Immenhauser et al., 2016), $\delta^{13}C_{shell}$ should show low values during the winter and higher values during the other months. This is because $\delta^{13}C_{DIC}$ values typically increase over spring and summer at shallow depths due to the preferential uptake of ^{12}C by photosynthesizers, and then progressively decrease over the rest of the year, as a result of respiratory return of isotopically light carbon to the DIC pool and low photosynthetic uptake (Lorrain et al., 2004). Thus, a supra-thermocline bivalve inheriting its shell carbon from DIC would show a pattern of seasonal variation in $\delta^{13}C_{shell}$ values opposite to that in $\delta^{18}O_{shell}$. By contrast, a sub-thermocline bivalve might be expected to show parallel variation of $\delta^{13}C_{shell}$ and $\delta^{18}O_{shell}$ values because DIC with a high ^{13}C content would only be available following the autumn breakdown of stratification and mixing down of surface waters (Johnson et al., 2021a). The interpretation that PJ2 lived at a greater depth compared to the other specimens is supported by the higher $\delta^{18}O$ values registered by its shell, which translate into lower water temperatures (Figs. 7, 8d). Such a discrepancy in water depth can be explained by time-averaging, which can condense in the same horizon fossils that lived at slightly different depths. In fact, fossiliferous levels in nearshore and shelf settings commonly form by the accumulation of shells over thousands to tens of thousands of years, an interval of time in which relative sea level can fluctuate (Flessa and Kowalewski, 1994; Kidwell, 1997). Presence, in the same outcrop, of shells that lived at different times and depth is supported by sedimentological evidence at the studied outcrop that points to a shoreface setting characterized by sediment starvation and condensation, with finer grained interbedding indicating short-term rises of fair-weather wave base (see Martini and Aldinucci, 2017). In contrast to PJ2, GL1, GL2, and PJ1 show the typical behaviour of supra-thermocline bivalves, with high $\delta^{13}C_{shell}$ values during the warmer months, and low $\delta^{13}C_{shell}$ values in winter (Figs. 3, 4). The same antiphase ontogenetic profiles can be observed in some modern *P. jacobaeus* shells collected from 25 and 30 m water depth (Peharda et al., 2019: Fig. 5).

Finally, although PJ3 shows a seasonal variation in $\delta^{18}O_{shell}$ values that covaries with the shape of micro-growth increment widths, it also shows a positive correlation between $\delta^{13}C_{shell}$ and $\delta^{18}O_{shell}$ values (Figs. 4, S10). Furthermore, the $\delta^{13}C_{shell}$ and $\delta^{18}O_{shell}$ values of PJ3 are lower compared to the other specimens, especially $\delta^{13}C_{shell}$ (Fig. 7). Depletion in $\delta^{13}C_{shell}$ is not rare and it is usually linked to metabolic sources through the introduction and incorporation of respiratory CO_2 into the shell (Owen et al., 2002b; Immenhauser et al., 2016). Also, changing relationships between $\delta^{13}C_{shell}$ and $\delta^{18}O_{shell}$ values in coeval specimens from the same habitat, both in modern and fossil examples, are often observed, and interpreted as reflecting biological controls on the incorporation of carbon isotopes into the shell (Lorrain et al., 2004; Peharda et al., 2019; Johnson et al., 2017).

5.2. Daily growth and growth rates of Pliocene G. latissimus and P. jacobaeus

While prominent growth lines are mostly associated with annual growth cycles, many subtidal bivalves form micro-growth increments daily (see Louis et al., 2022 for a review). However, this is not a rule. Concerning Pecitindae, some studies found a daily periodicity in the formation of striae (Clark II, 2005; Chauvaud et al., 1998, 2005), but others didn't. For instance, Owen et al. (2002a) showed that *P. maximus* formed daily striae only during the summer, the season that also coincided with the time during which the broadest micro-growth increments were formed, while striae production was less than one per day (down to <0.1 striae per day) during the rest of the year. A similar pattern was

observed for the species *Chlamys opercularis*, which formed daily micro-growth increments only when environmental conditions were favourable for growth, that is, during the summer (Broom and Mason, 1978). On top of that, the number of striae formed in one year is usually <365, also because bivalves can experience summer or winter cessation, or both (see Killam and Clapham, 2018), and the duration of the growing season decreases with age (Schöne and Surge, 2012), the very reason why it is important to compare specimens from the same ontogenetic stage, as we did. Table 1 shows clearly that the number of micro-growth increments counted in each annual cycle (identified by the presence of prominent growth lines and $\delta^{18}O_{shell}$ minima) of both *G. latissimus* and *P. jacobaeus* is far <365. To tentatively compare the growth rates of the two species we focused on the central part of each annual growth cycle, where the broadest micro-growth increments (wider than the average size in each cycle; Table 1) are formed, which have the highest probability of being formed daily according to the literature on modern specimens (e.g. Broom and Mason, 1978; Owen et al., 2002a). To estimate growth rate we selected only those micro-growth increments that occur in the central part of annual cycles, most of which are wider than the average micro-growth increment value of each annual cycle (Table S3). We used this approach only on available complete annual cycles for each specimen, which are year 2 and year 3 in GL1, year 2 in GL2 (Fig. 3), year 3 in PJ1 and year 2? In PJ3 (Fig. 4). By dividing the width of this interval of the shell by the number of observed striae, we estimate that *G. latissimus* grew around two times faster than *P. jacobaeus* (GL1 year 1: 508 μm/"day"; GL2 year 2: 648 μm/"day"; GL1 year 3: 527 μm/"day"; PJ1 year 3: 346 μm/"day"; PJ1 year2?: 299 μm/"day"), at least during the time of the year of formation of the widest micro-growth increments that coincides with low temperatures. We are aware that this is a partial estimate of growth rates, and that the two species could have had very different growth patterns when forming narrower micro-growth increments.

5.3. Extinction and survival at the demise of tropical marine conditions in the Mediterranean Sea

The available data, albeit derived from a few specimens that might not be representative of the entire variability of the species' adaptations, show that the growth strategies of *G. latissimus* and *P. jacobaeus* (for those specimens that lived above the thermocline) are typical of bivalves of subtropical affinity, as summer growth slow down and cessation typically occurs in modern bivalves that live between 15°- and 30° latitude (e.g. Ansell, 1968; Chauvaud et al., 1998; Hall et al., 1974; Tanabe and Oba, 1988; see Killam and Clapham, 2018 for a review). The Mediterranean Sea is located between 30° and 46° latitude, which is at the northern edge of such a latitudinal distribution. However, during most of the Pliocene, global climate was warmer than today (Salzmann et al., 2011, see also next paragraph), and the Mediterranean area was characterized by tropical-subtropical conditions (Suc et al., 2018).

In the late Zanclean-Piacenzian, the time interval of our studied specimens, average sea surface temperatures (SSTs) were warmer than today. This includes an interval of prolonged warmth, the mid-Piacenzian Warm Period (3.3–3.0 Ma; Dowsett et al., 2013), when mean SST was 1.8–3.6 °C higher than today (Haywood et al., 2020). According to some authors, tropical conditions extended south from the Peninsula of Setubal in southern Portugal (about 40° N) to the Canary (Raffi and Marasti, 1985; Monegatti and Raffi, 2001); according to others, tropical conditions extended to south of Cape Verde (Silva, da C. M., Landau, B., 2007; Ávila et al., 2016). In both scenarios, the Mediterranean area was included in the tropical belt. Over the time interval between 3.0 and 2.5 Ma there was a major shift in climate system involving increased climate variability, gradual cooling, and the intensification of Northern Hemisphere Glaciation, resulting in the appearance of large continental ice sheets over northern Eurasia and North America during two phases, at 2.7 and 2.5 Ma (Mudelsee and Raymo, 2005). In the Mediterranean basin, this interval can be regarded as a transitional period characterized by the emergence of a Mediterranean seasonal rhythm with summer drought and cooler winters, under more temperate conditions (Suc et al., 2018); the largest drop in SST was observed at c. 2.5 Ma (Herbert et al., 2015). Tropical conditions shrank in latitudinal extent to south of the Canary Islands, leaving a warm-temperate climate in the Mediterranean Sea. The onset of the cold Canary Current in the Atlantic, along the African coast, hindered the migration of species towards lower and warmer latitudes (Meco et al., 2020). This climate transition coincided with the extirpation from the Mediterranean Sea, or the global extinction, of many warm-adapted Pliocene species, including *G. latissimus* (Raffi and Marasti, 1985; Monegatti and Raffi, 2001; Danise and Dominici, 2023). Although *P. jacobaeus* was restricted to the Mediterranean Sea (only rare occurrences are found just outside Gibraltar: Rico-García, 2008) and had less probability of survival compared to eurythermal species living also in the North Atlantic and the North Sea (see Raffi and Marasti, 1985; Danise and Dominici, 2023), it survived climate and environmental change to the present. Raffi and Marasti (1985), hypothesised that the duration of summer temperatures necessary for reproduction was probably a key factor in controlling the extinction or survival of species at the Plio-Pleistocene transition.

Thermal stress is usually the main trigger of summer slowdown (or even cessation) of growth in bivalves that live under subtropical conditions, as they may not be able to adapt to the warmest temperatures (Killam and Clapham, 2018, and references therein). Even if there are no direct estimates of peak temperatures for the Mediterranean Pliocene, estimates based on the modern climate off the West African coast south of latitude 20–22° N, where a few Mediterranean Pliocene tropical survivors are found, suggest that mean monthly SSTs were probably over 24–25 °C for at least five to six months of the year (Monegatti and Raffi, 2001). Although the two investigated species had the same growth-adaptation to tropical-subtropical temperature, climate-environmental changes at the Plio-Pleistocene transition affected them in opposite ways, as one survived climate cooling while the other went extinct. Below we present some hypotheses that might explain such differential extinction.

The time of the year dedicated to spawning, and therefore the temperature at which it occurs, varies among species and strongly affects species survival (Vazquez et al., 2021). Field studies have suggested that a minimum threshold temperature or critical temperature range is necessary for spawning to occur in bivalves. The temperature that initiates spawning depends on acclimation history and can occur either with both increasing and decreasing temperatures (Barber and Blake, 2016). It has also been demonstrated that under increased thermal stress, bivalves may allocate energy away from growth and reproduction towards costly physiological defences to survive, and fecundity loss is one of the most likely consequences of that scenario (Petes et al., 2008) with, as an ultimate consequence, the decline or local extinction of populations (Parmesan, 2006). Different species of Pectinidae, like all marine bivalves, exhibit variation in gametogenic cycles. Gametogenesis can occur on an annual, semi-annual, or more continuous basis, when spawning takes place throughout the year (Barber and Blake, 2016). The few studies made on modern *P. jacobaeus* indicate that this species can spawn up to three times a year, in the spring, in the late summer/fall and in the winter (Castagnolo, 1991; Topić Popović et al., 2020; Ezgeta-Balić et al., 2022). Increased gametogenesis, shown by high values of the gonadosomatic index (GSI), during the late summer/fall interval coincides with the formation of the annual growth line, suggesting that *P. jacobaeus* transfers energy from shell growth to reproduction during this time of the year; by contrast, during the winter and spring, both growth rates and GSI values are high, indicating that *P. jacobaeus* has enough energy to sustain both shell growth and gametogenesis (Ezgeta-Balić et al., 2022). Although bivalves can modify their strategy of reproduction according to environmental conditions (e.g. at changing latitudes: Santos et al., 2011; Uribe et al., 2012), we hypothesize that the adaptation of *P. jacobaeus* to reproduce at different temperatures

through the year could have been one of the keys to its survival once sea water temperature decreased at the onset of the Northern Hemisphere glaciation. The evidence that *P. jacobaeus* is a eurythermal species with a wide bathymetric range (from 25 to 250 m; Poppe and Goto, 1993), as it was in the past (Danise and Dominici, 2023: Supplementary Material), supports the hypothesis that it can thrive and reproduce under a large range of temperatures.

Although *G. latissimus* show a similar life-habit, with summer slowdown, we observed that this species had higher growth rates compared to *P. jacobaeus*, at least when both species form broad micro-growth increments, which most likely formed daily (see above). Overall, bivalves of the genus *Gigantopecten* with their thick and large shells, had higher growth rates compared to most Pectinidae (Bongrain, 1988). In scallops, like in other ectotherms, metabolic rate is linearly correlated with temperature, as species with higher growth rates, and thus with higher metabolic costs, tend to live at higher temperature than species that have lower growth rates (Heilmayer et al., 2004). Therefore, *G. latissimus* might have had a narrower thermal range, and lower acclimatization potential compared to *P. jacobaeus* (see Pörtner et al., 2006). As there are no well-defined methods to distinguish with certainty, in the fossil record, spawning breaks on bivalve shells from breaks related to abiotic factors, it is difficult to infer the strategy of reproduction of *G. latissimus*, and how this could have impacted its survival. However, in some modern, tropical, large Pectinidae with summer growth-cessation (e.g. *Nodipecten subnodosus*, the largest tropical scallop), gametogenesis occurs in parallel with temperature rise, increasing towards the end of the summer, with spawning in the fall (Arellano-Martínez et al., 2011). If *G. latissimus* had a similar strategy, we can hypothesize that a decrease in summer temperature after 3.0 Ma might have inhibited gametogenesis, hampered its reproduction potential, and contributed to its extinction. Temperature might have also been an indirect driver of the extinction of *G. latissimus*. The *Gigantopecten* lineage diverged from the genus *Pecten* during the Early Miocene (Aquitanian-lower Burdigalian) or earlier (Bongrain, 1988). It developed gigantism to adapt to high-energy organogenic carbonate platforms that flourished during warm intervals of sea-level high stand (Bongrain, 1988). Large and thick shells, and several morphological characters (i.e., higher convexity of the left valves, nodes close to the umbo, low number of radial ribs), limit the movement of the shells under strong bottom currents and help to avoid burial (Bongrain, 1988). *G. latissimus* is the last known species of the genus, flourishing up to the mid-Piacenzian Warm Period (Dominici et al., 2020). The deterioration of climatic condition at the end of the Pliocene caused the reduction of shelf seas due to sea level fall and a massive decrease of organogenic substrates (Nalin et al., 2016; Cau et al., 2019). Such habitat loss and fragmentation could have also contributed to the extinction of the species (Bongrain, 1988; Danise and Dominici, 2023; Dominici and Danise, 2023). On top of this, whereas warm tropical surface waters are supersaturated with calcium carbonate and facilitate the production of thick shells, carbonate saturation decreases at lower seawater temperature, reducing the efficiency of shell formation (Watson et al., 2012).

Extinction of large, fast-growing bivalves during the Pliocene is not only documented from the Mediterranean Sea, but also from the Caribbean Sea (genus *Crassostrea*) and the western Atlantic coast (Pectinidae of the genera *Chesapecten* and *Carolinapecten*). Change in ocean circulation and planktonic productivity because of constriction and final closure of the Central American seaway has been invoked for the extinction of the giant oysters from the Caribbean Sea (Kirby and Jackson, 2004). We cannot exclude that, besides temperature, a change in primary productivity could have also impacted populations of *G. latissimus*, considering that is might have had high metabolic requirements. For instance, palaeogeographic and palaeoecological evidence suggest that nutrient-rich waters sustained during the Pliocene a high biomass of primary producers and a community of apex consumers and mesopredators, with a species-richness of cetaceans higher than the modern and a more complex trophic structure (Dominici et al., 2018). Such diversity is not documented during the Pleistocene (Dominici et al., 2020) and could be linked to a drop in primary production. The extinction of large western Atlantic scallops might have been also caused by the combined impact of declines in primary production and winter temperature, as the lower growth rate associated with these changes would have increased mortality through predation by preventing rapid achievement of the refuge offered by large size, causing a progressive reduction in overall population size (Johnson et al., 2019, 2021b). Analysis of the size of *G. latissimus* populations close to the timing of extinction, combined with an analysis of the evidence of predation (e.g. drill holes), might help in testing the possible role of increased predation pressure on its extinction.

5.4. Seawater palaeotemperature estimates

Limitations of our temperature reconstructions are mainly due to the uncertain estimate of $\delta^{18}O_{sw}$ values when our specimens formed their shells. For this reason, we chose a wide range (0.9–1.5 ‰), the lower estimate being the value previously applied for palaeotemperature reconstructions on a late Zanclean-early Piacenzian bivalve from the Siena-Radicofani Basin (Ragaini et al., 2019), the higher estimate being the value obtained from numerical models of Mediterranean Sea seawater during the mid-Piacenzian Warm Period (Tindall and Haywood, 2015; see also Material and Methods). We also assumed that $\delta^{18}O_{sw}$ values remained constant throughout the sampled seasons.

Ragaini et al. (2019) analysed through sclerochronology a valve of the infaunal venerid bivalve *Pelecyora gigas* from the same sedimentary basin of our specimens, and from a similar inner subtidal setting with a sandy bottom. Applying a $\delta^{18}O_{sw}$ value of 0.9 ‰ to the equation of Grossman and Ku (1986) for aragonite bivalves, an average temperature of 23 °C was obtained by Ragaini et al. (2019), with warm peaks up to 26–27 °C and cold temperatures down to 19–20 °C. For the same value of $\delta^{18}O_{sw}$, our minimum temperatures are substantially lower than those from *P. gigas* (minima of 14 °C), whereas our maximum temperatures are about the same (maxima up to 26 °C). Higher winter minima registered by *P. gigas* might be explained by winter-growth cessation for this extinct species, but more information on its growth pattern is needed to prove this hypothesis.

Additional estimates of the temperature of Pliocene Mediterranean Sea water come from other temperature proxies, especially from alkenones, organic molecules produced by coccolithophores, which allow reconstruction of SST in open ocean hemipelagic settings. Data from southern Italy indicate average SST of 25.5 °C between 3.5 and 2.6 Ma, with maximum values of 27–28 °C and minimum values down to 23.7 °C (Herbert et al., 2015; Beltran et al., 2021). Using a $\delta^{18}O_{sw}$ value of 1.5‰, our estimate of summer temperature is close to that derived from alkenones, but our minimum temperatures are substantially lower, with minima down to 17 °C and first percentile values down to 18–20 °C (Figs. 6, 7; excluding PJ2, which gives even colder estimates, see above). If, as recently shown, alkenone records are biased towards mean summer temperatures (Bova et al., 2021), our temperature estimate using the 1.5‰ value of $\delta^{18}O_{sw}$ seems to be the more reliable, as summer temperatures coincide using the two methods.

Help in interpreting our data comes from modern seasonal temperatures recorded in the Tyrrhenian Sea and in West Africa. Seasonal SSTs in the Tyrrhenian Sea for the years 1960–2017, reported in the ICOADS dataset, typically range between minimum values around 14 °C and maximum values of 26 °C, with peaks up to 27 °C (SNPA, 2018). Measurements near the Elba Island (northern Tyrrhenian Sea) in the years 2019–2022, include constant minimum winter temperatures of 14 °C at 5–25 m depth, and maximum summer temperatures that exceed 27 °C at 5 m depth and decrease 1 °C with every 5 m increase in depth (to 25 °C at 15 m, to 24 °C at 20 m, and to 23 °C at 25 m). Winter temperatures are thus constant through the depth gradient, while summer temperatures sharply decrease with depth (Azzola and Montefalcone, 2023). In Senegal, on the tropical western African coast, where a few

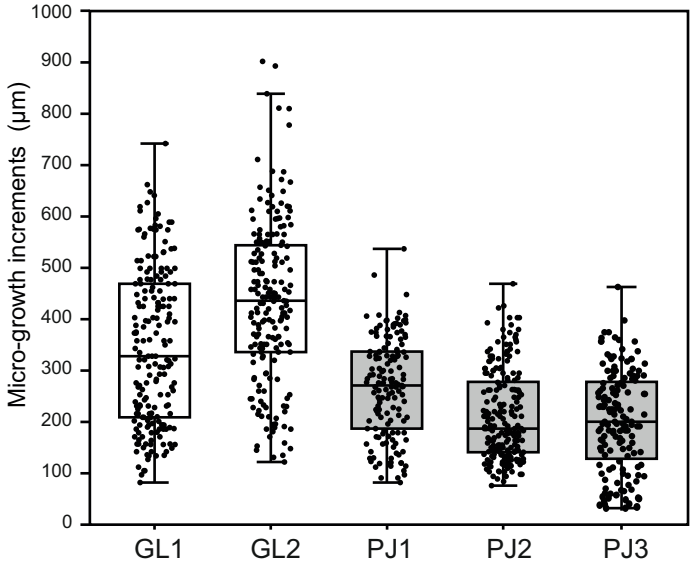

Fig. 6. Box plots of size variations of micro-growth increment widths for each specimen of *G. latissimus* and *P. jacobaeus*.

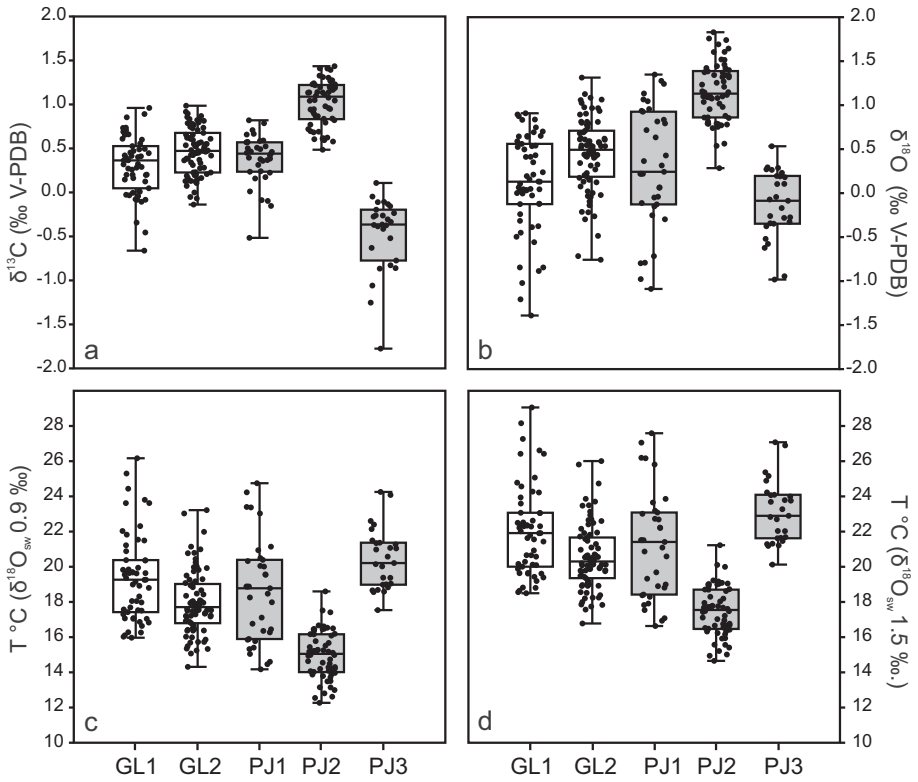

Fig. 7. Box plots showing variations of carbon and oxygen stable isotopes and palaeotemperature estimates. (a), $\delta^{13}C_{shell}$; (b) $\delta^{18}O_{shell}$; (c) palaeotemperatures for $\delta^{18}O_{sw}$ value of 0.9‰; (d) palaeotemperatures for $\delta^{18}O_{sw}$ value of 1.5 ‰, for the five studied specimens.

Mediterranean Pliocene tropical species still survive (Monegatti and Raffi, 2001), SST is instead 18–22 °C in the winter and 26.8–29.6 °C during summer (Huang et al., 2017). If, during the Pliocene interval here under study, climate conditions were comparable to those of West Africa, temperature estimates for a $\delta^{18}O_{sw}$ value of 1.5 ‰ would be again the most accurate, with minimum temperature of 16–17 °C, and maximum temperature of 28 °C or slightly higher (Fig. 7d, 8).

To avoid circular reasoning, additional proxies are needed to obtain temperature estimates with less uncertainty. For instance, experimental studies on modern species, like *P. jacobaeus*, combining $\delta^{18}O$ analyses with another independent palaeotemperature proxy from the same carbonate biomineral archive (e.g. Mg/Ca), could help to circumvent the main source of uncertainty in interpreting $\delta^{18}O$ palaeo-records: the value of $\delta^{18}O_{sw}$. This method, already successfully used for many other bivalves, including *Pecten maximus*, needs specific constraints as the equations are species-specific (Freitas et al., 2012). Alternatively, reliable temperature estimates could be obtained by combining clumped isotope (Δ_{47}) with $\delta^{18}O$ values, as recently done for Pliocene bivalves from the North Sea (Wichern et al., 2023). Such approaches would give not only more reliable reconstructions of past seasonal temperatures but

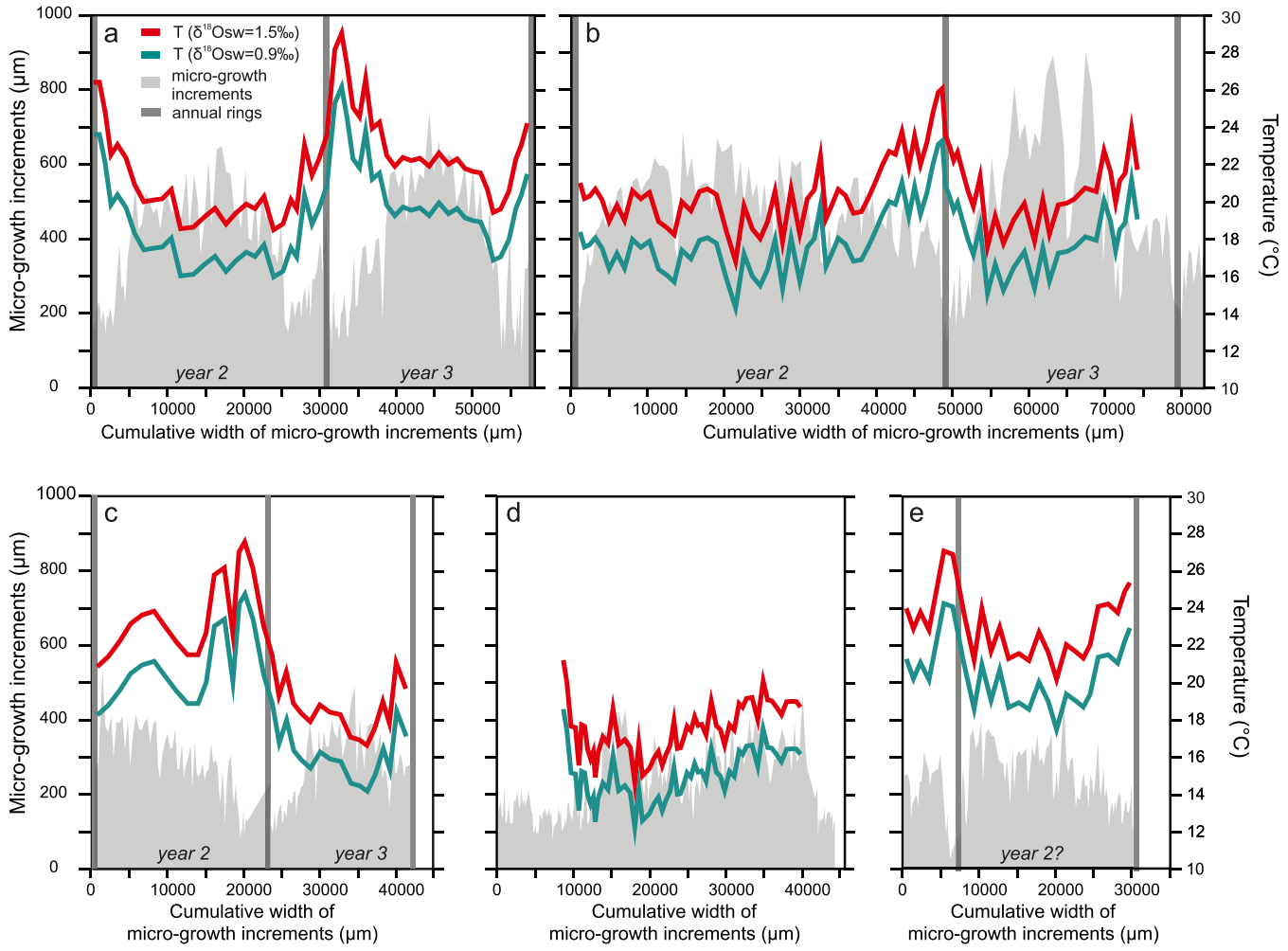

Fig. 8. Micro-growth increment widths and palaeotemperature estimates for $\delta^{18}O_{sw}$ of 0.9‰ and $\delta^{18}O_{sw}$ of 1.5‰ for *G. latissimus* (a: GL1; b: GL2) and *P. jacobaeus* (c: PJ1; d: PJ2; e: PJ3). Dark-grey vertical bars indicate visible annual growth lines on the surface of the shell.

would also shed light on the adaptation and plasticity of species, like *Pecten jacobaeus*, thriving under different climate regimes. For instance, modern *P. jacobaeus* in the Adriatic Sea sharply decreases its growth during summer at temperatures higher than 20 °C, and its shell does not record temperatures higher than 22 °C (Ezgeta-Balić et al., 2022), while during the Pliocene it could withstand higher temperatures. This provides a perspective on whether populations will be able to adapt to future warming (e.g. Parmesan, 2006), although other evidence suggests that the scope for rapid adjustment to adjust the individual energy budget to changing temperature is rather limited for scallops (Heilmayer et al., 2004). Models of the future distribution of Mediterranean Sea endemic species, including *P. jacobaeus*, predict substantial range contractions and fragmentation, leading to complete extinction by end-century of most endemic species, given the fast rate of global change (Gallagher and Albano, 2023).

6. Conclusions

In this study we applied a sclerochronological approach to compare the growth patterns of two species from the Pliocene of the Mediterranean Sea, the extinct *Gigantopecten latissimus* and the extant *Pecten jacobaeus*. Our aim was to investigate whether such an approach would help in better understanding the causes of the extinction of the former and the survival of the latter due to climate and other environmental changes linked to the onset of the Northern Hemisphere Glaciation. We then used seasonally constrained oxygen isotope values from the shells to estimate absolute palaeotemperatures for the Tyrrhenian Sea during the late Zanclean-Piacenzian.

Our dataset is small, and analysing a larger number of specimens would have allowed a more robust reconstruction of the life-habit of the studied species, given that environmental and climate conditions influence shell growth, and that the latter vary on inter-annual and decadal time-scales. From the data available so far, we can conclude that, for those specimens that lived above the thermocline and were influenced by surface waters, the two species had very similar seasonal growth patterns, characterized by summer slowdown, with a brief shutdown, often not at the temperature peak. Such behaviour is typical of subtropical species that decrease their growth around summer temperature maxima because of thermal stress. We also estimated that *G. latissimus* had higher growth rates compared to *P. jacobaeus* (at least during the colder months, when micro-growth increments possibly formed daily). This could have implied higher metabolic costs and possibly narrower thermal limits for *G. latissimus*. We hypothesised that higher costs might have been no longer sustainable under a colder climate regime and could have contributed to its extinction. Further analyses, with a higher number of specimens and longer time-series of $\delta^{18}O_{shell}$ $\delta^{13}C_{shell}$ values, will help testing this hypothesis. A second driver to consider, when advancing hypotheses to explain the extinction of *G. latissimus* and the survival of *P. jacobaeus*, is the strategy of reproduction, in terms of timing of spawning, usually strongly influenced by temperature in bivalves. Modern *P. jacobaeus* shows a high versatility in reproduction, as it can spawn up to three times a year,

during different seasons. Possibly *G. latissimus* had a more specialised adaptation (i.e., spawning only once per year when temperature reached its maximum values), like some modern pectinids from tropical waters, characterized by a similarly very large size. This cannot be verified because it was not possible in this study to distinguish spawning breaks from breaks linked to abiotic factors in fossil shells. Climate change might have also played an indirect role in the extinction of *G. latissimus* in the form of habitat loss and fragmentation due to the reduction of shelf seas resulting from sea level fall, a massive decrease of organogenic substrates, and the onset of the cold Canary Current on the western African coast, interrupting the connection with southern tropical areas.

Comparison of fossil and recent *P. jacobaeus* from the Mediterranean Sea indicates that Pliocene specimens lived and reproduced under warmer conditions, and this opens the question on the potential adaptation of modern populations of *P. jacobaeus* to future warming scenarios.

Temperature estimates from fossil shells indicate a Pliocene climate in the Mediterranean Sea with winter minima down to 18 °C and summer maxima up to 29 °C, when applying a $\delta^{18}O_{sw}$ value of 1.5‰; this temperature regime is comparable to that of the west Africa tropical belt. However, integrated sclerochronological analysis of modern and fossil specimens, combining different geochemical proxies (i.e., $\delta^{18}O$, Mg/Ca, Δ_{47}), would allow the production of more reliable reconstructions of past seasonal temperatures.

Funding

Italian Ministry for University and Research, Grant Programma per Giovani Ricercatori “Rita Levi Montalcini” to S. Danise.

CRediT authorship contribution statement

Silvia Danise: Writing – review & editing, Writing – original draft, Methodology, Investigation, Funding acquisition, Formal analysis, Conceptualization. **Giada Giachetti:** Writing – review & editing, Writing – original draft, Investigation, Formal analysis. **Ilaria Baneschi:** Writing – review & editing, Writing – original draft, Resources, Investigation, Formal analysis, Conceptualization. **Martina Casalini:** Writing – review & editing, Writing – original draft, Resources, Investigation, Formal analysis. **Francesco Miniati:** Writing – review & editing, Writing – original draft, Methodology, Investigation, Formal analysis. **Stefano Dominici:** Writing – review & editing, Writing – original draft, Data curation. **Chiara Boschi:** Writing – review & editing, Writing – original draft, Resources, Investigation, Formal analysis, Conceptualization.

Declaration of competing interest

The authors declare that they have no known competing financial interests or personal relationships that could have appeared to influence the work reported in this paper.

Data availability

Al used data are available in the Supplementary Material

Acknowledgments

The authors thank M. Ghinassi for providing the location of origin of the specimens. Thanks to J. McArthur for providing the up-to-date LOESS look-up table of values of $^{87}Sr/^{86}Sr$ for dating our samples, and to M. Belvedere for the helpful discussions. We are also thankful to three anonymous reviewers for their detailed and insightful suggestions.

Appendix A. Supplementary data

Supplementary data to this article can be found online at https://doi.org/10.1016/j.palaeo.2024.112429.

References

Aguirre, J., Braga, J.C., Jiménez, A.P., Rivas, P., 1996. Substrate-related changes in pectinid fossil assemblages. Palaeogeogr. Palaeoclimatol. Palaeoecol. 126, 291–308.

Anderson, T.F., Arthur, M.A. (1983) Stable isotopes of oxygen and carbon and their application to sedimentologic and paleoenvironmental problems, in: Arthur, M.A., et al. (Eds.), Stable isotopes in sedimentary geology: Society of Economic Paleontologists and Mineralogists Short Course 10, pp. 1–151.

Ansell, A.D., 1968. The rate of growth of the hard clam *Mercenaria mercenaria* (L) throughout the geographical range. ICES J. Mar. Sci. 31, 364–409.

Arellano-Martínez, M., Ceballos-Vázquez, B.P., Ruíz-Verdugo, C., Perez de Leon, E., Cervantes-Duarte, R., Domínguez-Valdéz, P.M., 2011. Growth and reproduction of the lion's paw scallop *Nodipecten subnodosus* in a suspended culture system at Guerrero Negro lagoon, Baja California Sur. Mexico. Aquacul. Res. 42 (4), 571–582.

Arthur, M.A., Williams, D.F., Jones, D.S., 1983. Seasonal temperature-salinity changes and thermocline development in the mid-Atlantic Bight as recorded by the isotopic composition of bivalves. Geology 11, 655–659.

Avanzinelli, R., Boari, E., Conticelli, S., Francalanci, L., Guarnieri, L., Perini, G., Petrone, C.M., Tommasini, S., Ulivi, M., 2005. High precision Sr, Nd, and Pb isotopic analyses using the new generation thermal ionisation mass spectrometer ThermoFinnigan Triton-Ti®. Periodico di Mineralogia 74, 147–166.

Ávila, S.P., Ramalho, R.S., Habermann, J.M., Quartau, R., Kroh, A., Berning, B., Johnson, M., Kirby, M.X., Zanon, V., Titschack, J., Goss, A., 2015. Palaeoecology, taphonomy, and preservation of a lower Pliocene shell bed (coquina) from a volcanic oceanic island (Santa Maria Island, Azores). Palaeogeogr. Palaeoclimatol. Palaeoecol. 430, 57–73.

Ávila, S.P., Melo, C., Berning, B., Cordeiro, R., Landau, B., da Silva, C.M., 2016. *Persististrombus coronatus* (Mollusca: Strombidae) in the lower Pliocene of Santa Maria Island (Azores, NE Atlantic): paleoecology, paleoclimatology and paleobiogeographic implications. Palaeogeogr. Palaeoclimatol. Palaeoecol. 441, 912–923.

Azzola, A., Montefalcone, M., 2023. Relazione del terzo anno di progetto mare caldo (2021−2022). Monitoraggio degli effetti dei cambiamenti climatici sugli ecosistemi marini bentonici di scogliera, Report Greenpeace-Distav, 70 pages. https://www.greenpeace.org/static/planet4-italy-stateless/2021/05/c4ee04c8-distav_relazione-mare-caldo-primo-anno-2019-2020_23.04.2021.pdf.

Backman, J., Raffi, I., Rio, D., Fornaciari, E., Pälike, H., 2012. Biozonation and biochronology of Miocene through Pleistocene calcareous nannofossils from low and middle latitudes. Newsl. Stratigr. 45, 221–244.

Barber, B.J., Blake, N.J., 2016. Reproductive Physiology. In: Shumway, S.E., Parsons, G. J. (Eds.), Scallops: Biology, Ecology, Aquaculture, and Fisheries. Elsevier, Third Edition, pp. 252–292.

Barbin, V., Schein, E., Roux, M., Decrouez, D., Ramseyer, K., 1991. Stries de croissance révéléespar cathodoluminescence dans la coquille de *Pecten maximus* (L.) récent de la rade de Brest (Pectinidae, Bivalvia). Geobios 24 (1), 65–70.

Beltran, C., Sicre, M.A., Ohneiser, C., Sainz, M., 2021. A composite Pliocene record of sea surface temperature in the Central Mediterranean (Capo Rossello composite section–South Sicily). Sediment. Geol. 420, 105921.

Bice, K.L., Arthur, M.A., Marincovich Jr., L., 1996. Late Paleocene Arctic Ocean shallow-marine temperatures from mollusc stable isotopes. Paleoceanography 11 (3), 241–249.

Bongrain, M., 1988. Les *Gigantopecten* (Pectinidae, Bivalvia) du Miocène français. Croissance, morphogenèse, paléoécologie. Cahiers Paléonl. Paris, p. 270.

Bongrain, M., 1992. Le rôle des hétérochronies du développement dans l'apparition et la différenciation des gigantopecten (Pectinidae, Bivalvia) néogènes: esquisse de la phylogénie du groupe. Geobios 25, 77–85.

Bonini, M., Sani, F., 2002. Extension and compression in the Northern Apennines (Italy) hinterland: evidence from the late Miocene-Pliocene Siena-Radicofani Basin and relations with basement structures. Tectonics 21 (3), 1–35.

Borges, P.A.V., Costa, A., Cunha, R., Gabriel, R., Gonçalves, V., Martins, A.F., Melo, I., Parente, M., Raposeiro, P., Rodrigues, P., Santos, R.S., Silva, L., Vieira, P., Vieira, V., 2010. A list of the terrestrial and marine biota from the Azores, 432 pp. Chapter 14: Lista de invertebrados marinhos costeiros. Ed A.C. Costa. in Princípia, Oeiras, pp. 287–324.

Bossio, A., Costantini, A., Lazzarotto, A., Liotta, D., Mazzanti, R., Mazzei, R., Salvatorini, G.F., Sandrelli, F., 1993. Rassegna delle conoscenze sulla stratigrafia del Neoautoctono toscano. Mem. Soc. Geol. Ital. 49, 17–98.

Bova, S., Rosenthal, Y., Liu, Z., Godad, S.P., Yan, M., 2021. Seasonal origin of the thermal maxima at the Holocene and the last interglacial. Nature 589 (7843), 548–553.

Brand, U., Veizer, J., 1980. Chemical diagenesis of a multicomponent carbonate system-1: minor elements. J. Sediment. Res. 50, 1219–1236.

Briard, J., Pucéat, E., Vennin, E., Daëron, M., Chavagnac, V., Jaillet, R., de Merle, D., Rafélis, M., 2020. Seawater paleotemperature and paleosalinity evolution in neritic environments of the Mediterranean margin: Insights from isotope analysis of bivalve shells. Palaeogeogr. Palaeoclimatol. Palaeoecol. 543, 109582.

Brocchi, G.B., 1814. Conchologia fossile subapennina, con osservazioni geologiche sugli Apennini e sul suolo adiacente. Stamperia Reale, Milano.

Brogi, A., 2011. Bowl-shaped basin related to low-angle detachment during continental extension: the case of the controversial Neogene Siena Basin (Central Italy, Northern Apennines). Tectonophysics 499 (1–4), 54–57.
Broom, M.J., Mason, J., 1978. Growth and spawning in the pectinid *Chlamys opercularis* in relation to temperature and phytoplankton concentration. Mar. Biol. 47, 277–285.
Carmignani, L., Decandia, F.A., Disperati, L., Fantozzi, P.L., Kligfield, R., Lazzarotto, A., Liotta, D., Meccheri, M., 2001. Inner Northern Apennines. In: Vai, G.B., Martini, I.P. (Eds.), Anatomy of an Orogene. Kluwer Academic Publishers, The Apennines and Adjacent Mediterranean Basins, pp. 197–214.
Carter, J.G., 1990. Evolutionary significance of shell microstructure in the Palaeotaxodonta, Pteriomorphia and Isofilibranchia (Bivalvia: Mollusca). In: Carter, J.G. (Ed.), Skeletal Biomineralisation: Patterns, Processes and Evolutionary Trends, vol. 1. Van Nostrand Reinhold, New York, pp. 135–296.
Castagnolo, L., 1991. La pesca e la riproduzione di *Pecten jacobaeus* L. e di *Aequipecten opercularis* (L.) nell'Alto Adriatico. Bollettino Malacol. 27, 39–48.
Cau, S., Laini, A., Monegatti, P., Roveri, M., Scarponi, D., Taviani, M., 2019. Palaeocological anatomy of shallow-water Plio-Pleistocene biocalcarenites (northern Apennines, Italy). Palaeogeogr. Palaeoclimatol. Palaeoecol. 514, 838–851.
Chauvaud, L., Thouzeau, G., Paulet, Y.M., 1998. Effects of environmental factors on the daily growth rate of Pecten maximus juveniles in the Bay of Brest (France). J. Exp. Mar. Biol. Ecol. 227 (1), 83–111.
Chauvaud, L., Lorrain, A., Dunbar, R.B., Paulet, Y.M., Thouzeau, G., Jean, F., Guarini, J. M., Mucciarone, D., 2005. Shell of the Great Scallop *Pecten maximus* as a high-frequency archive of paleoenvironmental changes. Geochem. Geophys. Geosyst. 6 (8), Q08001.
Chauvaud, L., Thébault, J., Clavier, J., Lorrain, A., Strand, Ø., 2011. What's hiding behind ontogenetic $\delta^{13}C$ variations in mollusk shells? New insights from the Great Scallop (*Pecten maximus*). Estuar. Coasts 34, 211–220.
Chauvaud, L., Patry, Y., Jolivet, A., Cam, E., Le Goff, C., Strand, Ø., Charrier, G., Thébault, J., Lazure, P., Gotthard, K., Clavier, J., 2012. Variation in size and growth of the Great Scallop *Pecten maximus* along a latitudinal gradient. PLoS One 7 (5), e37717.
Clark II, G.R., 1974. Growth lines in invertebrate skeletons. Annu. Rev. Earth Planet. Sci. 2 (1), 77–99.
Clark II, G.R., 2005. Daily growth lines in some living Pectens (Mollusca: Bivalvia), and some applications in a fossil relative: time and tide will tell. Palaeogeogr. Palaeoclimatol. Palaeoecol. 228 (1–2), 26–42.
Coll, M., Piroddi, C., Steenbeek, J., Kaschner, K., Ben Rais Lasram, F., Aguzzi, J., Ballesteros, E., Bianchi, C.N., Corbera, J., Dailianis, T., Danovaro, R., 2010. The biodiversity of the Mediterranean Sea: estimates, patterns, and threats. PLoS One 5 (8), e11842.
Colleoni, F., Cherchi, A., Masina, S., Brierley, C.M., 2015. Impact of global SST gradients on the Mediterranean runoff changes across the Plio-Pleistocene transition. Paleoceanography 30 (6), 751–767.
Dämmer, L.K., de Nooijer, L., van Sebille, E., Haak, J.G., Reichart, G.J., 2020. Evaluation of oxygen isotopes and trace elements in planktonic foraminifera from the Mediterranean Sea as recorders of seawater oxygen isotopes and salinity. Clim. Past 16 (6), 2401–2414.
Danise, S., Dominici, S., 2023. Biodiversity change and extinction risk in Plio-Pleistocene Mediterranean bivalves: the families Veneridae, Pectinidae and Lucinidae. Geol. Soc. Lond. Spec. Publ. 529 (1), SP529–2022.
Dominici, S., Danise, S., 2023. Mediterranean onshore–offshore gradient in the composition and temporal turnover of benthic molluscs across the middle Piacenzian warm Period. Geol. Soc. Lond. Spec. Publ. 529 (1), SP529–2022.
Dominici, S., Danise, S., Benvenuti, M., 2018. Pliocene stratigraphic paleobiology in Tuscany and the fossil record of marine megafauna. Earth Sci. Rev. 176, 277–310.
Dominici, S., Danise, S., Cau, S., Freschi, A., 2020. The awkward record of fossil whales. Earth Sci. Rev. 205, 103057.
Dowsett, H.J., Robinson, M.M., Stoll, D.K., Foley, K.M., Johnson, A.L., Williams, M., Riesselman, C.R., 2013. The PRISM (Pliocene palaeoclimate) reconstruction: time for a paradigm shift. Phil. Trans. R. Soc. A 371 (2001), 20120524.
Ezgeta-Balić, D., Peharda, M., Schöne, B.R., Uvanović, H., Vrgoč, N., Markulin, K., Radonić, I., Denamiel, C., Kovač, Ž., 2022. Different life strategies of the three commercially exploited scallop species living under the same environmental conditions. Front. Mar. Sci. 9, 992042 https://doi.org/10.3389/fmars.2022.992042.
Fatton, E., 1973. De la province biogéographique à la population d'après les Pectinidés néogènes et actuels. Centre d'Études et de Recherches de Paléontologie biostratigraphique (CERPAB). Notes et Contributions 3, 1–213.
Fauquette, S., Suc, J.P., Jiménez-Moreno, G., Micheels, A., Jost, A., Favre, E., Bachiri-Taoufiq, N., Bertini, A., Clet-Pellerin, M., Diniz, F., Farjanel, G., 2007. Latitudinal climatic gradients in the Western European and Mediterranean regions from the Mid-Miocene (c. 15 Ma) to the Mid-Pliocene (c. 3.5 Ma) as quantified from pollen data. In: Williams, M., Haywood, A.M., Gregory, F.J., Schmidt, D.N. (Eds.), Deep-Time Perspectives on Climate Change: Marrying the Signal from Computer Models and Biological Proxies. The Micropalaeontological Society, Special Publications. The Geological Society, London, pp. 481–502.
Flessa, K.W., Kowalewski, M., 1994. Shell survival and time-averaging in nearshore and shelf environments: estimates from the radiocarbon literature. Lethaia 27 (2), 153–165.
Freitas, P.S., Clarke, L.J., Kennedy, H., Richardson, C.A., 2012. The potential of combined Mg/ca and $\delta^{18}O$ measurements within the shell of the bivalve *Pecten maximus* to estimate seawater $\delta^{18}O$ composition. Chem. Geol. 291, 286–293.
Freneix, S., Saint Martin, J.-P., Moissette, P., 1987. Bivalves Ptériomorphes du Messinien d'Oranie (Algérie occidentale). Bulletin du Muséum National d'Histoire Naturelle 4 (1), 3–61.
Gallagher, K.M., Albano, P.G., 2023. Range contractions, fragmentation, species extirpations, and extinctions of commercially valuable molluscs in the Mediterranean Sea—a climate warming hotspot. ICES J. Mar. Sci. fsad065.
García-Ramos, D.A., Zuschin, M., 2019. High-frequency cycles of brachiopod shell beds on subaqueous delta-scale clinoforms (early Pliocene, south-East Spain). Sedimentology 66 (5), 1486–1530.
Ghinassi, M., Ielpi, A., 2018. Morphodynamics and facies architecture of streamflow-dominated, sand-rich alluvial fans, Pleistocene Upper Valdarno Basin, Italy. Geol. Soc., London Spec. Publ. 440 (1), 175–200.
Goewert, A.E., Surge, D., 2008. Seasonality and growth patterns using isotope sclerochronology in shells of the Pliocene scallop *Chesapecten madisonius*. Geo-Mar. Lett. 28 (5), 327–338.
Gofas, S., Luque, Á.A., Templado, J., Salas, C., 2017. A national checklist of marine Mollusca in Spanish waters. Sci. Mar. 81 (2), 241–254.
Goodwin, D.H., Schöne, B.R., Dettman, D.L., 2003. Resolution and fidelity of oxygen isotopes as paleotemperature proxies in bivalve mollusk shells: models and observations. Palaios 18 (2), 110–125.
Grossman, E.L., Ku, T.L., 1986. Oxygen and carbon isotopic fractionation in biogenic aragonite: temperature effects. Chem. Geol. 59, 59–74.
Hall, C.A., Dollase, W.A., Corbatò, C.E., 1974. Shell growth in *Tivela stultorum* (Mawe, 1823) and *Callista chione* (Linnaeus, 1758) (Bivalvia): annual periodicity, latitudinal differences, and diminution with age: Palaeogeography. Palaeoclimatol., Palaeoecol. 15, 33–61.
Harzhauser, M., Mandic, O., Zuschin, M., 2003. Changes in Paratethyan marine molluscs at the early/Middle Miocene transition: diversity, palaeogeography and palaeoclimate. Acta Geol. Pol. 53 (4), 323–339.
Hayami, I., Hosoda, I., 1988. *Fortipecten takahashii*, a reclining pectinid from the Pliocene of North Japan. Palaeontology 31, 419–444.
Haywood, A.M., Sellwood, B.W., Valdes, P.J., 2000. Regional warming: Pliocene (3 Ma) paleoclimate of Europe and the Mediterranean. Geology 28 (12), 1063–1066.
Haywood, A.M., Tindall, J.C., Dowsett, H.J., Dolan, A.M., Foley, K.M., Hunter, S.J., Hill, D.J., Le Chan, W., Abe-Ouchi, A., Stepanek, C., Lohmann, G., Chandan, D., Richard Peltier, W., Tan, N., Contoux, C., Ramstein, G., Li, X., Zhang, Z., Guo, C., Nisancioglu, K.H., Zhang, Q., Li, Q., Kamae, Y., Chandler, M.A., Sohl, L.E., OttoBliesner, B.L., Feng, R., Brady, E.C., Von Der Heydt, A.S., Baatsen, M.L.J., Lunt, D.J., 2020. The Pliocene model intercomparison project phase 2: large-scale climatefeatures and climate sensitivity. Clim. Past 16, 2095e2123. https://doi.org/10.5194/cp-16-2095-2020.
Heilmayer, O., Brey, T., Pörtner, H.O., 2004. Growth efficiency and temperature in scallops: a comparative analysis of species adapted to different temperatures. Funct. Ecol. 18, 641–647.
Herbert, T.D., Ng, G., Peterson, L.C., 2015. Evolution of Mediterranean Sea surface temperatures 3.5–1.5 Ma: regional and hemispheric influences. Earth Planet. Sci. Lett. 409, 307–318.
Huang, B., Peter, W., Thorne, P.W., Banzon, V.F., Boyer, T., Chepurin, G., Lawrimore, J. H., Menne, M.J., Smith, T.M., Vose, R.S., Zhang, H.-M., 2017. NOAA Extended Reconstructed Sea Surface Temperature (ERSST), Version 5. NOAA National Centers for Environmental Information. https://doi.org/10.7289/V5T72FNM.
Iacumin, P., Bianucci, G., Longinelli, A., 1992. Oxygen and carbon isotopic composition of fish otoliths. Mar. Biol. 113, 537–542.
Immenhauser, A., Nägler, T.F., Steuber, T., Hippler, D., 2005. A critical assessment of mollusk $^{18}O/^{16}O$, Mg/Ca, and $44^{Ca}/^{40}Ca$ ratios as proxies for cretaceous seawater temperature seasonality. Palaeogeogr. Palaeoclimatol. Palaeoecol. 215 (3–4), 221–237.
Immenhauser, A., Schöne, B.R., Hoffmann, R., Niedermayr, A., 2016. Mollusc and brachiopod skeletal hard parts: Intricate archives of their marine environment. Sedimentology 63 (1), 1–59.
Ivany, L.C., Lohmann, K.C., Hasiuk, F., Blake, D.B., Glass, A., Moody, R.M., 2008. Eocene climate record of a high southern latitude continental shelf: Seymour Island, Antarctica. Bull. Geol. Soc. Am. 120, 659–678.
Jiménez, A.P., Aguirre, J., Rivas, P., 2009. Taxonomic study of scallops (Pectinidae: mollusca, bivalvia) from Pliocene deposits (Almería, SE Spain). Spanish J. Palaeontol. 24 (1), 1–30.
Jochum, K.P., Nohl, U., Herwig, K., Lammel, E., Stoll, B., Hofmann, A.W., 2005. GeoReM: a new geochemical database for reference materials and isotopic standards. Geostand. Geoanal. Res. 29 (3), 333–338.
Johnson, A.L.A., Hickson, J.A., Swan, J., Brown, M.R., Heaton, T.H.E., Chenery, S., Balson, P.S., 2000. The Queen Scallop *Aequipecten opercularis*: a new source of information on late Cenozoic marine environments in Europe. Geol. Soc. Lond. Spec. Publ. 177 (1), 425–439.
Johnson, A.L., Valentine, A., Leng, M.J., Sloane, H.J., Schöne, B.R., Balson, P.S., 2017. Isotopic temperatures from the early and Mid-Pliocene of the US Middle Atlantic Coastal Plain, and their implications for the cause of regional marine climate change. Palaios 32 (4), 250–269.
Johnson, A.L.A., Valentine, A.M., Leng, M.J., Schöne, B.R., Sloane, H.J., 2019. Life history, environment and extinction of the scallop *Carolinapecten eboreus* (Conrad) in the Plio-Pleistocene of the U.S. eastern seaboard. Palaios 34, 49–70.
Johnson, A.L.A., Harper, E.M., Clarke, A., Featherstone, A.C., Heywood, D.J., Richardson, K.E., Spink, J.O., Thornton, L.A.H., 2021a. Growth rate, extinction and survival amongst late Cenozoic bivalves of the North Atlantic. Hist. Biol. 33 (6), 802–813.
Johnson, A.L., Valentine, A.M., Schöne, B.R., Leng, M.J., Sloane, H.J., Janeković, I., 2021b. Growth-increment characteristics and isotopic ($\delta^{18}O$) temperature record of sub-thermocline *Aequipecten opercularis* (Mollusca: Bivalvia): evidence from modern Adriatic forms and an application to early Pliocene examples from eastern England. Palaeogeogr. Palaeoclimatol. Palaeoecol. 561, 110046.

Jones, D.S., Allmon, W.D., 1995. Records of upwelling, seasonality and growth in stable-isotope profiles of Pliocene mollusk shells from Florida. Lethaia 28 (1), 61–74.
Jones, D.S., Arthur, M.A., Allard, D.J., 1989. Sclerochronological records of temperature and growth from shells of *Mercenaria mercenaria* from Narragansett Bay, Rhode Island. Mar. Biol. 102, 225–234.
Jost, A., Fauquette, S., Kageyama, M., Krinner, G., Ramstein, G., Suc, J.P., Violette, S., 2009. High resolution climate and vegetation simulations of the late Pliocene, a model-data comparison over western Europe and the Mediterranean region. Clim. Past 5 (4), 585–606.
Kidwell, S.M., 1997. Time-averaging in the marine fossil record: Overview of strategies and uncertainties. Geobios 30 (7), 977–995.
Killam, D.E., Clapham, M.E., 2018. Identifying the ticks of bivalve shell clocks: seasonal growth in relation to temperature and food supply. Palaios 33 (5), 228–236.
Kirby, M.X., Jackson, J.B., 2004. Extinction of a fast-growing oyster and changing ocean circulation in Pliocene tropical America. Geology 32 (12), 1025–1028.
Lartaud, F., Emmanuel, L., De Rafélis, M., Ropert, M., Labourdette, N., Richardson, C.A., Renard, M., 2010. A latitudinal gradient of seasonal temperature variation recorded in oyster shells from the coastal waters of France and the Netherlands. Facies 56, 13–25.
Linnaeus, C., 1758. Systema Naturae per Regna Tria Naturae, Secundum Classes, Ordines, Genera, Species, Cum Characteribus, Differentiis, Synonymis, Locis, Editio decima, reformata [10th revised edition], 1. Laurentius Salvius, Stockholm, p. 824.
Lorrain, A., Paulet, Y.M., Chauvaud, L., Dunbar, R., Mucciarone, D., Fontugne, M., 2004. $\delta^{13}C$ variation in scallop shells: increasing metabolic carbon contribution with body size? Geochim. Cosmochim. Acta 68 (17), 3509–3519.
Louis, V., Besseau, L., Lartaud, F., 2022. Step in time: Biomineralisation of bivalve's shell. Front. Mar. Sci. 9, 906085.
Mandic, O., Piller, W.E., 2001. Pectinid coquinas and their palaeoenvironmental implications – examples from the early Miocene of northeastern Egypt. Palaeogeogr. Palaeoclimatol. Palaeoecol. 172, 171–191.
Mariotti, A., Struglia, M.V., Zeng, N., Lau, K., 2002. The hydrological cycle in the Mediterranean region and implications for the water budget of the Mediterranean Sea. J. Clim. 15 (13), 1674–1690.
Marshall, J.D., 1992. Climatic and oceanographic isotopic signals from the carbonate rock record and their preservation. Geol. Mag. 129, 143–160.
Martini, E., 1971. Standard Tertiary and Quaternary calcareous nannoplankton zonation, in: Farinacci, a. In: (Ed.), Proceedings 2nd International Conference Planktonic Microfossils Roma: Rome (Ed. Tecnosci.) 2, pp. 739–785.
Martini, I., Aldinucci, M., 2017. Sedimentation and basin-fill history of the Pliocene succession exposed in the northern Siena-Radicofani Basin (Tuscany, Italy): a sequence-stratigraphic approach. Riv. Ital. Paleontol. Stratigr. 123 (3), 407–432.
Martini, I.P., Sagri, M., 1993. Tectono-sedimentary characteristics and the genesis of the recent magmatism of Southern Tuscany and Northern Latium. Periodico di Mineralogia 56, 157–172.
Martini, I., Aldinucci, M., Foresi, L.M., Mazzei, R., Sandrelli, F., 2011. Geological map of the Pliocene succession of the Northern Siena Basin (Tuscany, Italy). J. Maps 7 (1), 193–205.
Martini, I., Foresi, L.M., Bambini, A.M., Riforgiato, F., Ambrosetti, E., Sandrelli, F., 2016. Calcareous plankton bio-chronostratigraphy and sedimentology of the "I Sodi" section (Siena Basin, Italy): a key section for the uppermost Neogene marine deposition in the inner northern Apennines. Ital. J. Geosci. 135 (3), 540–547.
Martini, I., Ambrosetti, E., Brogi, A., Aldinucci, M., Zwaan, F., Sandrelli, F., 2021. Polyphase extensional basins: interplay between tectonics and sedimentation in the Neogene Siena-Radicofani Basin (Northern Apennines, Italy). Int. J. Earth Sci. 110 (5), 1729–1751.
Mason, J., 1957. The age and growth of the scallop, *Pecten maximus* (L.), in Manx waters. J. Mar. Biol. Assoc. U. K. 36 (3), 473–492.
McArthur, J.M., Howarth, R.J., Shields, G.A., Zhou, Y., 2020. Strontium isotope stratigraphy, chapter 7. In: Gradstein, F.M., Ogg, J.G., Schmitz, M.D., Ogg, G.M. (Eds.), Geologic Time Scale. Elsevier, pp. 211–238.
Meco, J., Lomoschitz, A., Koppers, A.A., Miggins, D.P., Huertas, M.J., Betancort, J.F., Soler-Onis, E., 2020. Late Miocene and early Pliocene coastal deposits from the Canary Islands: New records and paleoclimatic significance. J. Afr. Earth Sci. 164, 103802.
Mondanaro, A., Dominici, S., Danise, S., 2024. Response of Mediterranean Sea bivalves to Pliocene-Pleistocene environmental change. Palaeontology 67, e12696.
Monechi, S., Thierstein, H.R., 1985. Late Cretaceous-Eocene nannofossil and magnetostratigraphic correlations near Gubbio, Italy. Mar. Micropaleontol. 9, 419–440.
Monegatti, P., Raffi, S., 2001. Taxonomic diversity and stratigraphic distribution of Mediterranean Pliocene bivalves. Palaeogeogr. Palaeoclimatol. Palaeoecol. 165, 171–193.
Morvezen, R., Charrier, G., Boudry, P., Chauvaud, L., Breton, F., Strand, O., Laroche, J., 2016. Genetic structure of a commercially exploited bivalve, the great scallop *Pecten maximus*, along the European coasts. Conserv. Genet. 17 (1), 57–67.
Moss, D.K., Ivany, L.C., Judd, E.J., Cummings, P.W., Bearden, C.E., Kim, W.J., Artruc, E. G., Driscoll, J.R., 2016. Lifespan, growth rate, and body size across latitude in marine Bivalvia, with implications for Phanerozoic evolution. Proc. R. Soc. B 283 (1836), 20161364.
Moss, D.K., Ivany, L.C., Jones, D.S., 2021. Fossil bivalves and the sclerochronological reawakening. Paleobiology 47 (4), 551–573.
Mudelsee, M., Raymo, M.E., 2005. Slow dynamics of the Northern Hemisphere glaciation. Paleoceanography 20 (4), PA4022. https://doi.org/10.1029/2005PA001153.
Nalin, R., Ghinassi, M., Foresi, L.M., Dallanave, E., 2016. Carbonate Deposition in Restricted Basins: a Pliocene Case Study from the Central Mediterranean (Northwestern Apennines), Italy. J. Sediment. Res. 86, 236–267.
Okada, H., Bukry, D., 1980. Supplementary modification and introduction of code numbers to the low-latitude coccolith biostratigraphic zonation (Bukry 1973, 1975). Mar. Micropaleontol. 5, 321–325.
Owen, R., Richardson, C., Kennedy, H., 2002a. The influence of shell growth rate on striae deposition in the scallop *Pecten maximus*. J. Mar. Biol. Assoc. U. K. 82 (4), 621–623.
Owen, R., Kennedy, H., Richardson, C., 2002b. Experimental investigation into partitioning of stable isotopes between scallop (*Pecten maximus*) shell calcite and sea water. Palaeogeogr. Palaeoclimatol. Palaeoecol. 185, 163–174.
Parmesan, C., 2006. Ecological and evolutionary responses to recent climate change. Annu. Rev. Ecol. Evol. Syst. 37, 637–669.
Pascucci, V., Martini, I.P., Sagri, M., Sandrelli, F., 2007. Effects of the transverse structural lineaments on Neogene-Quaternary basin of Tuscany (inner Northern Apennines, Italy). In: Nichols, G., Paola, C., Williams, E.A. (Eds.), Sedimentary Processes, Environments and Basins - a Tribute to Peter Friend. Special Publication, IAS, p. 37.
Peharda, M., Soldo, A., Pallaoro, A., Matic, S., Cetinic, P., 2003. Age and growth of the Mediterranean scallop *Pecten jacobaeus* (Linnaeus 1758) in the Northern Adriatic Sea. J. Shellfish Res. 22 (3), 639–642.
Peharda, M., Thébault, J., Markulin, K., Schöne, B.R., Janeković, I., Chauvaud, L., 2019. Contrasting shell growth strategies in two Mediterranean bivalves revealed by oxygen-isotope ratio geochemistry: the case of *Pecten jacobaeus* and *Glycymeris pilosa*. Chem. Geol. 526, 23–35.
Peharda, M., Schöne, B.R., Black, B.A., Correge, T., 2021. Advances of sclerochronology research in the last decade. Palaeogeogr. Palaeoclimatol. Palaeoecol. 570, 110371.
Petes, L.E., Menge, B.A., Harris, A.L., 2008. Intertidal mussels exhibit energetic tradeoffs between reproduction and stress resistance. Ecol. Monogr. 78, 387–402.
Pierre, C., 1999. The oxygen and carbon isotope distribution in the Mediterranean water masses. Mar. Geol. 153, 41–55.
Poppe, G.T., Goto, Y., 1993. European Seashells. 2 (Scaphopoda, Bivalvia, Cephalopoda. ConchBooks, Hackenheim.).
Poppe, G.T., Goto, Y., 2000. European Seashells, Volume II. Scaphopoda, Bivalvia.
Pörtner, H.O., Bennett, A.F., Bozinovic, F., Clarke, A., Lardies, M.A., Lucassen, M., Pelster, B., Schiemer, F., Stillman, J.H., 2006. Trade-offs in thermal adaptation: the need for a molecular to ecological integration. Physiol. Biochem. Zool. 79, 295–313.
Raffi, S., Stanley, S.M, Marasti, R. (1985). Biogeographic patterns and Plio-Pleistocene extinction of Bivalvia in the Mediterranean and Southern North Sea. Paleobiology 11, 368–388.
Ragaini, L., Ficini, F., Zanchetta, G., Regattieri, E., Perchiazzi, N., Dallai, L., 2019. Mineralogy and oxygen isotope profile of *Pelecyora gigas* (Veneridae, Bivalvia) from Tuscan Pliocene. Alpine Med. Quater. 32 (1), 5–13.
Richardson, C.A., 2001. Molluscs as archives of environmental change. Oceanogr. Mar. Biol. 39, 103–164.
Rico-García, A., 2008. Pectínidos pliocenos de la Cuenca de Vejer (Cádiz, SO de España). Studia Geologica Salmanticensia 44, 91–140.
Roux, M., Schein, E., Rio, M., Davanzo, F., Filly, A., 1990. Enregistrement des paramètres du milieu et des phases de croissance par les rapports $^{18}O/^{16}O$ et $^{13}C/^{12}C$ dans la coquille de *Pecten maximus* (Pectinidae, Bivalvia). Comptes rendus de l'Académie des sciences Paris Série 2 (310), 385–390.
Saavedra, C., Peña, J.B., 2004. Phylogenetic relationships of commercial European and Australasian scallops (*Pecten* spp.) based on partial 16S ribosomal RNA gene sequences. Aquaculture 235, 153–166.
Saavedra, C., Peña, J.B., 2005. Nucleotide diversity and Pleistocene population expansion in Atlantic and Mediterranean scallops (*Pecten maximus* and *P. Jacobaeus*) as revealed by the mitochondrial 16S ribosomal RNA gene. J. Exp. Mar. Biol. Ecol. 323 (2), 138–150.
Salzmann, U., Williams, M., Haywood, A.M., Johnson, A.L., Kender, S., Zalasiewicz, J., 2011. Climate and environment of a Pliocene warm world. Palaeogeogr. Palaeoclimatol. Palaeoecol. 309, 1–8.
Santos, S., Cardoso, J.F.M.F., Carvalho, C., Luttikhuizen, P.C., van der Veer, H.W., 2011. Seasonal variability in somatic and reproductive investment of the bivalve *Scrobicularia plana* (da Costa, 1778) along a latitudinal gradient. Estuar. Coast. Shelf Sci. 92, 19–26.
Schein, E., Roux, M., Barbin, V., Chiési, F., Renard, M., Rio, M., 1991. Enregistrement des paramétres écologiques par la coquille des bivalves: Approche pluridisciplinaire. Bulletin de la Société géologique de France. 162, 687–698.
Schmidt, G.A., 1998. Oxygen-18 variations in a global ocean model. Geophys. Res. Lett. 25, 1201–1204.
Schöne, B.R., 2008. The curse of physiology—challenges and opportunities in the interpretation of geochemical data from mollusk shells. Geo-Mar. Lett. 28, 269–285.
Schöne, B.R., Surge, D.M., 2012. Part N, revised, volume 1, chapter 14: Bivalve sclerochronology and geochemistry. Treatise online 46, 1–24.
Silva, da C.M., Landau, B., 2007. Cenozoic Atlanto-Mediterranean biogeography of *Spiricella* (Gastropoda, Umbraculidae) and climate change: filling the geological gap. Veliger 49, 19–26.
SNPA, 2018. Rapporto Ambiente. In: Doc. n. 07/2019, SNPA, Rapporti 07_2019, Roma, p. 345. ISBN 978-88-448-0943-0.
Studencka, B., 2019. Note on *Gigantopecten nodosiformis* (Pusch, 1837), the logo of the 8th International Workshop on Neogene of Central and South-Eastern Europe. NCSEE 2019. In: 8th International Workshop on Neogene of Central and South-Eastern Europe, pp. 12–13. Abstract Volume, Chęciny, Poland.
Suc, J.P., Popescu, S.M., Fauquette, S., Bessedik, M., Jiménez-Moreno, G., Bachiri Taoufiq, N., Zheng, Z., Medail, F., Klotz, S., 2018. Reconstruction of Mediterranean

flora, vegetation and climate for the last 23 million years based on an extensive pollen dataset. Ecologia Mediterranea 44, 53–85.
Surge, D., Lohmann, K.C., Dettman, D.L., 2001. Controls on isotopic chemistry of the American oyster, *Crassostrea virginica*: Implications for growth patterns. Palaeogeogr. Palaeoclimatol. Palaeoecol. 172, 283–296.
Tanabe, K., Oba, T. (1988). Latitudinal variation in shell growth patterns of *Phacosoma japonicum* (Bivalvia: Veneridae) from the Japanese coast. Marine Ecology Progress Series47, 75–82.
Taylor, J.D., Kennedy, W.J., Hall, A., 1969. The Shell Structure and Mineralogy of the Bivalvia, Introduction. Nuculacea – Trigonacea. Bulletin of the British Museum (Natural history). Zoology Supplement 3, 125.
Thirlwall, M.F., 1991. Long-term reproducibility of multicollector Sr and Nd isotope ratio analysis. Chem. Geol. 94, 85–104.
Tindall, J.C., Haywood, A.M., 2015. Modeling oxygen isotopes in the Pliocene: Large-scale features over the land and ocean. Paleoceanography 30 (9), 1183–1201.
Topić Popović, N., Beer Ljubić, B., Strunjak-Perović, I., Babić, S., Lorencin, V., Jadan, M., Čižmek, L., Matulić, D., Bojanić, K., Čož-Rakovac, R., 2020. Seasonal antioxidant and biochemical properties of the Northern Adriatic *Pecten jacobaeus*. PLoS One 15 (3), e0230539.
Ullmann, C.V., Korte, C., 2015. Diagenetic alteration in low-Mg calcite from macrofossils: a review. Geological Quarterly 59, 3–20.
Uribe, R.A., Oliva, M.E., Aguilar, S., Yamashiro, C., Riascos, J.M., 2012. Latitudinal variation in the reproductive cycle of two bivalves with contrasting biogeographical origin along the Humboldt Current Upwelling Ecosystem. Sci. Mar. 76, 713–720.
Vazquez, E., Woodin, S.A., Wethey, D.S., Peteiro, L.G., Olabarria, C., 2021. Reproduction under stress: acute effect of low salinities and heat waves on reproductive cycle of four ecologically and commercially important bivalves. Front. Mar. Sci. 8, 685282.
Waller, T.R., 1991. Evolutionary relationships among commercial scallops (Mollusca: Bivalvia: Pectinidae), in: Shumway, S.E. (Ed.), Scallops: biology, ecology and aquaculture. Develop. Aquacult. Fish. Sci., Elsevier, Amsterdam 21, 1–73.
Walliser, E.O., Lohmann, G., Niezgodzki, I., Tütken, T., Schöne, B.R., 2016. Response of central European SST to atmospheric pCO2 forcing during the Oligocene–a combined proxy data and numerical climate model approach. Palaeogeogr. Palaeoclimatol. Palaeoecol. 459, 552–569.
Ward, L.W., Blackwelder, B.W. (1975). *Chesapecten*, a new genus of Pectinidae (Mollusca: Bivalvia) from the Miocene and Pliocene of eastern North America. Geological Survey Professional Paper 861, iv, 24 pp., 27 pls.
Watson, S.A., Peck, L.S., Tyler, P.A., Southgate, P.C., Tan, K.S., Day, R.W., Morley, S.A., 2012. Marine invertebrate skeleton size varies with latitude, temperature and carbonate saturation: implications for global change and ocean acidification. Glob. Chang. Biol. 18 (10), 3026–3038.
Wefer, G., Berger, W.H., 1991. Isotope paleontology: growth and composition of extant calcareous species. Mar. Geol. 100, 207–248.
Weidman, C.R., Jones, G.A., 1994. The long-lived mollusc *Arctica islandica*: a new paleoceanographic tool for the reconstruction of bottom temperatures for the continental shelves of the northern North Atlantic Ocean. J. Geophys. Res. 99 (C9), 18.305-18.314.
Wichern, N.M., de Winter, N.J., Johnson, A.L., Goolaerts, S., Wesselingh, F., Hamers, M. F., Kaskes, P., Claeys, P., Ziegler, M., 2023. The fossil bivalve *Angulus benedeni benedeni*: a potential seasonally resolved stable-isotope-based climate archive to investigate Pliocene temperatures in the southern North Sea basin. Biogeosciences 20 (12), 2317–2345.
Wierzbowski, H., 2021. Advances and challenges in palaeoenvironmental studies based on oxygen isotope composition of skeletal carbonates and phosphates. Geosciences 11 (10), 419.
Wilding, C.S., Beaumont, A.R., Latchford, J.W., 1999. Are *Pecten maximus* and *Pecten jacobaeus* different species? J. Mar. Biol. Assoc. U. K. 79, 949–952.
Williams, M., Nelson, A.E., Smellie, J.L., Leng, M.J., Johnson, A.L., Jarram, D.R., Haywood, A.M., Peck, V.L., Zalasiewicz, J., Bennett, C., Schöne, B.R., 2010. Sea ice extent and seasonality for the early Pliocene northern Weddell Sea. Palaeogeogr. Palaeoclimatol. Palaeoecol. 292, 306–318.
Zachos, J.C., Stott, L.D., Lohmann, K.C., 1994. Evolution of early Cenozoic marine temperatures. Paleoceanography 9, 353–387.